The Effect of Meridional and Vertical Shear on the Interaction of Equatorial Baroclinic and Barotropic Rossby Waves

By Joseph A. Biello and Andrew J. Majda

Simplified asymptotic equations describing the resonant nonlinear interaction of equatorial Rossby waves with barotropic Rossby waves with significant midlatitude projection in the presence of arbitrary vertically and meridionally sheared zonal mean winds are developed. The three mode equations presented here are an extension of the two mode equations derived by Majda and Biello [1] and arise in the physically relevant regime produced by seasonal heating when the vertical (baroclinic) mean shear has both symmetric and antisymmetric components; the dynamics of the equatorial baroclinic and both symmetric and antisymmetric barotropic waves is developed. The equations described here are novel in several respects and involve a linear dispersive wave system coupled through quadratic nonlinearities. Numerical simulations are used to explore the effect of antisymmetric baroclinic shear on the exchange of energy between equatorial baroclinic and barotropic waves; the main effect of moderate antisymmetric winds is to shift the barotropic waves meridionally. A purely meridionally antisymmetric mean shear yields highly asymmetric waves which often propagate across the equator. The two mode equations appropriate to Ref. [1] are shown to have analytic solitary wave solutions and some representative examples with their velocity fields are presented.

Address for correspondence: Dr. Joseph A. Biello, Courant Institute of Mathematical Sciences, 251 Mercer Street, New York, NY, 10012; e-mail: biello@cims.nyu.edu

STUDIES IN APPLIED MATHEMATICS 112:341–390

Published by Blackwell Publishing, 350 Main Street, Malden, MA 02148, USA, and 9600 Garsington Road, Oxford, OX4 2DQ, UK.

1. Introduction

Energy exchange in the troposphere between the equatorial region and midlatitudes is a topic of considerable interest for understanding global teleconnection patterns from the tropics to midlatitudes as well as the midlatitude influence on such tropical wave dynamics as monsoons, the Madden–Julian intraseasonal oscillation and El Niño. An important theoretical issue is the exchange of energy between equatorially trapped baroclinic waves and barotropic waves with a significant projection on the midlatitudes. To gain basic insight into the fashion in which tropical heating generates a midlatitude response, Webster [2–4] utilized a two-layer global primitive equation model and Kasahara and Silva Dias [5] did analogous studies with a linearized global primitive equation model. Both studies showed that localized, steady forcing of baroclinic waves in the tropics can drive a large, rapid response in barotropic waves with a significant projection at midlatitudes when the zonal averaged winds have both vertical and meridional shears. Hoskins and Jin [6] similarly studied the transient response to localized tropical forcing of midlatitude barotropic waves. This work again confirmed the role of vertical and horizontal shears and further emphasized the importance of nearly dispersionless equatorial Rossby waves in generating midlatitude barotropic waves. Wang and Xie [7] performed a linear stability analysis for an equatorial β-plane two-layer model around basic zonal states with both meridional and vertical shear. Their results showed that at large scales, $m = 1$, equatorial Rossby waves strongly coupled to barotropic waves in the midlatitudes as linearized characteristic modes of propagation provided that there is vertical shear in the zonal background state; furthermore, the dispersion relation of the long wavelength, $m = 1$, equatorial Rossby waves at large scales is modified significantly by the presence of a mean vertical shear. Regarding the forcing of the tropics by midlatitude waves, Lim and Chang [8, 9] have suggested the importance of vertical mean shear for a significant response while Hoskins and Yang [10] have emphasized the role of nearly resonant forcing in several specific physical mechanisms. Recently Lin et al. [11] showed the significance of midlatitude dynamics in triggering tropical intraseasonal responses in an intermediate climate model with essentially two vertical modes of resolution; a barotropic mode and a baroclinic heating mode.

These results inspired Majda and Biello [1] to develop a nonlinear model describing the interaction of equatorial Rossby waves and barotropic waves with a significant midlatitude projection in a theory where nonlinear advection is the only nonlinearity. Beginning with a two layer β-plane model as in Webster [2–4] and Wang and Xie [7], Majda and Biello [1] derive asymptotic equations governing the interaction of long equatorial baroclinic and barotropic waves in the presence of zonal mean shears; the long wave scaled equatorial baroclinic-barotropic (LWSEBB) equations. These equations contain nearly

dispersionless long wave solutions that are able to resonantly interact and exchange energy. Exploiting this resonant interaction, the authors [1] developed a small amplitude theory of nearly dispersionless, long equatorial baroclinic and symmetric barotropic waves in the presence of baroclinic and barotropic shear with the same meridional structure as their respective waves; the reduced equations for equatorial baroclinic-barotropic waves (REEBBW). These waves are coupled through vertical shear (baroclinic zonal means), horizontal shear (barotropic and baroclinic zonal means) and nonlinearly through wave–wave interaction. It is shown in [1] that while the REBBW equations are derived through a weakly nonlinear theory, the amplitude expansion parameter, ϵ, is the Froude number and conservative values of $\epsilon = 0.1$ yield atmospherically relevant wind velocities and wave speeds. Using these equations Majda and Biello demonstrate that energy exchange between equatorial Rossby waves and barotropic waves with significant midlatitude projection is greatly aided by the presence of vertical shear and occurs within 12 days for climatologically appropriate mean winds and shears.

The present work expands on Ref. [1] by considering the small amplitude theory of the LWSEBB in the presence of arbitrary mean baroclinic and barotropic shears. This situation is important physically since off-equatorial seasonal heating typically produces such asymmetric zonal shears. In particular, the presence of baroclinic mean shear with the opposite symmetry of the baroclinic waves couples the original baroclinic and symmetric barotropic waves to an antisymmetric barotropic wave. After a brief recapitulation of the LWSEBB in Section 2, the reduced equations

$$\begin{aligned} 0 &= A_\tau - DA_{xxx} + \mu A_x + \Gamma_S B^S_x + \Gamma_A B^A_x + (AB^S)_x \\ 0 &= B^S_\tau - B^S_{xxx} + \Gamma_S A_x + \lambda B^S_x + \sigma B^A_x + AA_x \\ 0 &= B^A_\tau - B^A_{xxx} + \Gamma_A A_x + \sigma B^S_x - \lambda B^A_x \end{aligned} \tag{1}$$

governing the resonant interaction of equatorial baroclinic (A) and symmetric and antisymmetric barotropic waves (B^S, B^A) in the presence of arbitrary baroclinic and barotropic zonal mean shears are derived in Section 3. Under different physical assumptions in the context of midlatitude baroclinic instability, Mitsudera [12] and Gottwald and Grimshaw [13] recently derived models using a weak β effect and resonant interaction which yielded pairs of KdV equations with nonlinear self-interaction but only linear coupling, in contrast to Ref. [1] and the Equations (1).

The equations derived here are novel in both atmospheric sciences and applied mathematics having both linear energy exchange in the presence of zonal mean shears and nonlinear baroclinic-barotropic wave coupling. In Section 4 the energy properties, Hamiltonian structure and physical interpretation of the amplitude equations are discussed. The presence of antisymmetric baroclinic shear yields mean zonal velocities whose maxima are meridionally shifted and

the antisymmetric barotropic waves allow the possibility of tilted vortices. Because the equations are an extension of the theory derived in Ref. [1], it is important to consider how the presence of antisymmetric baroclinic shear affects the energy exchange between barotropic and baroclinic waves. In Section 5, numerical solutions of the amplitude equations are presented which describe the effect of antisymmetric baroclinic shear and antisymmetric barotropic winds on the interaction of barotropic and baroclinic waves. In Section 6 we present analytic solitary wave solutions to the original equations derived in Ref. [1] which are a specific case of the present model. These explicit solutions provide interesting solitary waves in the presence of suitable mean shears in the tropics to demonstrate various effects. The velocity fields of the solitary waves and their stability under collisions are also described.

2. The long wave scaled equatorial baroclinic-barotropic equations

The LWSEBB equations were derived by Majda and Biello [1] and form the basis of our discussion here. For completeness we briefly summarize their derivation.

The two-layer, nondimensionalized equatorial β-plane equations for the barotropic and baroclinic horizontal velocity and pressure, $\vec{v}_0$, p_0 and $\vec{v}_1$, p_1, respectively are given by

$$\frac{\bar{D}}{Dt}\vec{v}_0 + y\vec{v}_0^{\perp} + \vec{v}_1 \mathrm{div}\,(\vec{v}_1) + (\vec{v}_1 \cdot \nabla)\vec{v}_1 = -\nabla p_0$$
$$\mathrm{div}\,\vec{v}_0 = 0 \tag{2}$$

$$\frac{\bar{D}}{Dt}\vec{v}_1 + y\vec{v}_1^{\perp} + (\vec{v}_1 \cdot \nabla)\,\vec{v}_0 = -\nabla p_1$$
$$\frac{\bar{D}}{Dt}p_1 + \mathrm{div}\,\vec{v}_1 = 0. \tag{3}$$

In (2) and (3) $\vec{v}_j = (u_j, v_j)$, $\vec{v}_j^{\perp} = (-v_j, u_j)$, p_j for $j = 1, 2$ are functions of the horizontal variable, (x, y) alone and all the vector derivatives involve only horizontal differentiation. Here and elsewhere in the paper the transport operator $\frac{\bar{D}}{Dt} = \frac{\partial}{\partial t} + \vec{v}_0 \cdot \nabla$ represents advection by the barotropic mode. The nonlinear equations for the interaction of barotropic and baroclinic modes in (2), (3) can be derived in standard fashion [14, 15] from a two-vertical-mode Galerkin truncation of the Boussinesq equations on the β-plane with rigid lid boundary conditions of the form

$$\vec{v} = \vec{v}_0 + \vec{v}_1\sqrt{2}\cos\left(\frac{\pi z}{H}\right)$$
$$p = p_0 + p_1\sqrt{2}\cos\left(\frac{\pi z}{H}\right) \tag{4}$$

where $c = \frac{H\bar{N}}{\pi}$ is the corresponding gravity wave speed determined by the Brunt–Vaisala frequency, $\bar{N} = 10^{-2}s^{-1}$, and the troposphere thickness, H. In (2) and (3) the equations have been nondimensionalized through the units of length measured by the equatorial Rossby radius, $L_E = (c/\beta)^{1/2}$ and time given by $T_E = (c\beta)^{-1/2}$ while velocity and pressure are nondimensionalized by c and c^2, respectively. Below, the standard values associated with dry wave propagation of an equatorial baroclinic heating mode with

$$c = 50 \text{ m s}^{-1}, \quad T_E = 8.3 \text{ h}, \quad L_E = 1500 \text{ km} \tag{5}$$

are utilized to demonstrate various qualitative effects of the nonlinear coupling in (2), (3). Note that the total energy of both barotropic and baroclinic modes,

$$\begin{aligned} E &= \frac{1}{2}\int |\vec{v}_0|^2 + \frac{1}{2}\int |\vec{v}_1|^2 + |p_1|^2 \\ &= E_{BT} + E_{BC} \end{aligned} \tag{6}$$

is conserved by (2) and (3).

Using a stream function, ψ, satisfying $u_0 = -\psi_y$, $v_0 = \psi_x$, the barotropic Equations in (2) are reduced to an equivalent scalar equation for ψ by taking the curl of the first equation in (2). The result is the equation

$$\frac{\bar{D}}{Dt}\Delta\psi + \psi_x + \text{div}\left(-(\vec{v}_1 u_1)_y + (\vec{v}_1 v_1)_x\right) = 0. \tag{7}$$

In the linear theory of equatorial baroclinic and barotropic equations, (2) and (7) are well known to admit nearly dispersionless waves of long azimuthal wavelength [16, 20]. To capture solely the interaction of these equatorial baroclinic Rossby waves and barotropic Rossby waves we perform a long zonal wave scaling for the coupled equations in (3) and (7). Zonal variations in x are assumed to occur on the longer basic length scale, L, with corresponding weaker meridional velocities and a longer basic unit of time, T, satisfying

$$\frac{L_E}{L} = \delta, \quad \frac{T_E}{T} = \delta, \quad |v| = \delta|u| \tag{8}$$

for $\delta \ll 1$. Assume that the solutions of interest for (3) and (7) vary on scales compatible with (8); thus, in the original nondimensional units, assume

$$\begin{aligned} \psi &= \psi(\delta x, y, \delta t), \quad p_1 = p_1(\delta x, y, \delta t) \\ u_1 &= u_1(\delta x, y, \delta t), \quad v_1 = \delta v_1(\delta x, y, \delta t). \end{aligned} \tag{9}$$

For solutions with the special form (9), the equations in (3) and (7) become the LWSEBB equations

$$\frac{\bar{D}}{Dt}u_1 - \vec{v}_1 \cdot \nabla \psi_y - yv_1 + (p_1)_x = 0$$
$$\frac{\bar{D}}{Dt}p_1 + \operatorname{div}(\vec{v}_1) = 0 \tag{10}$$
$$(p_1)_y + yu_1 + \delta^2 \left(\frac{\bar{D}}{Dt}v_1 + \vec{v}_1 \cdot \nabla \psi_x \right) = 0$$

and

$$\frac{\bar{D}}{Dt}(\psi_{yy}) + \psi_x - \operatorname{div}\left((\vec{v}_1 u_1)_y\right) + \delta^2 \left(\frac{\bar{D}}{Dt}(\psi_{xx}) + \operatorname{div}\left((\vec{v}_1 v_1)_x\right) \right) = 0 \tag{11}$$

which were derived in Ref. [1]. To avoid cumbersome notation, the arguments of the variables displayed in (9) are written implicitly in (10) and (11) and are still denoted by x, y, t in Section 3.

2.1. Linear theory of LWSEBB

To leading order in δ, the LWSEBB equations in (10) and (11) linearized about a zero background state reduce to the decoupled linear equatorial long-wave equation [16, 20] and the linear barotropic long-wave equations, respectively. The linear barotropic long-wave equation has the well-known dispersion relation, $\omega_{BT} = -\frac{k}{l^2}$, with corresponding dispersionless Rossby wave train solutions,

$$\psi = -B^S(x - c_{BT}t)\sin(ly) - B^A(x - c_{BT}t)\cos(ly), \quad c_{BT} = -\frac{1}{l^2} \tag{12}$$

for any wavenumber l. The superscripts "S" and "A" denote waves whose zonal velocity, $u = -\psi_y$, is symmetric or antisymmetric about the equator, respectively. The essential difference between this work and Ref. [1] is the inclusion of the antisymmetric barotropic mode and, in particular, its interesting interaction through the mean shear with the symmetric barotropic and equatorial baroclinic waves.

Similarly, the linear equatorial long-wave equation, (10), has dispersionless equatorial Rossby wavetrain solutions [16, 20]

$$\begin{pmatrix} p \\ u \\ v \end{pmatrix} = \begin{pmatrix} -\frac{A_m(x - c_m t)}{\sqrt{2}}\left(D_{m-1} + \frac{D_{m+1}}{(m+1)}\right) \\ \frac{A_m(x - c_m t)}{\sqrt{2}}\left(D_{m-1} - \frac{D_{m+1}}{(m+1)}\right) \\ -\left(\frac{2}{2m+1}\right)\frac{\partial A_m(x - c_m t)}{\partial x} D_m \end{pmatrix} \tag{13}$$

for any integer $m > 0$ where $D_m(y)$ are the parabolic cylinder functions and

$$c_m = -\frac{1}{2m+1}. \tag{14}$$

The baroclinic waves have symmetric zonal velocity about the equator for m odd and antisymmetric zonal velocity for m even and decay exponentially away from the equator.

For a fixed m, the dispersionless packets in (12) and (13) are resonant for a barotropic mode with meridional wavelength, L_* with $l = \frac{2\pi}{L_*} L_E$ provided that

$$c_{BT}(L_*) = c_m \Longrightarrow l = \sqrt{2m+1} \quad \text{or} \quad \frac{L_*}{L_E} \equiv L = \frac{2\pi}{\sqrt{2m+1}} \tag{15}$$

for $m = 1, 2, 3, \ldots$ With the gravity wave speed, $c = 50\ \mathrm{m\,s^{-1}}$ and $L_E = 1500$ km from (5) the dimensional meridional wavelengths of the resonant barotropic Rossby waves are approximately

$$\begin{aligned} L_* &\cong 3.6 L_E = 5440 \text{ km} \quad \text{for} \quad m = 1 \\ L_* &\cong 2.8 L_E = 4200 \text{ km} \quad \text{for} \quad m = 2 \end{aligned} \tag{16}$$

so that the barotropic Rossby wavetrains have a substantial projection at midlatitudes for $m = 1, 2$.

3. Amplitude equations for the LWSEBB

Majda and Biello [1] derived amplitude equations for the interaction of equatorial Rossby and barotropic waves in the presence of mean shear. In that model the mean shear was conserved by the dynamics, so too in the model derived below. Importantly, the derivation assumed that the baroclinic mean shear had the same meridional symmetry as the baroclinic waves. In particular the examples considered in Ref. [1] corresponded to $m = 1$ symmetric baroclinic waves coupled to $l = \sqrt{3}$ symmetric barotropic waves where the baroclinic mean shear and barotropic mean wind are also symmetric about the equator. In such an instance the antisymmetric barotropic modes evolve solely through linear dispersion, not interacting with the symmetric barotropic or baroclinic waves. However, as we shall show, a baroclinic shear of opposite meridional symmetry of the baroclinic waves provides an additional mechanism for energy exchange with antisymmetric barotropic waves, which is the main focus of this paper.

We are interested in the resonant interaction, from Equation (15), of barotropic waves (12) and baroclinic waves (13) through a mean barotropic zonal wind, $U_{BT} = -\bar{\psi}_y(y)$, mean baroclinic vertical shear, $\bar{U}(y)$, and its corresponding pressure, $\bar{P}(y)$. Geostrophic balance requires that the baroclinic mean velocity and pressure be related through

$$\bar{P}_y + y\bar{U} = 0 \tag{17}$$

which is just the equatorial baroclinic Equation (2) for steady, zonally constant winds. Motivated by (12), (13), and (15) we seek small amplitude weakly

nonlinear wave/mean flow solutions of the LWSEBB equations

$$\begin{aligned}
\psi &= -\epsilon B^S(x - c_m t, \epsilon t)\sin(ly) - \epsilon B^A(x - c_m t, \epsilon t)\cos(ly) \\
&\quad + \epsilon\bar{\psi}(y) + \epsilon^2\psi_2(x, y, t, \epsilon t) \\
p_{BC} &= -\epsilon\frac{A(x - c_m t, \epsilon t)}{\sqrt{2}}\left(D_{m-1} + \frac{D_{m+1}}{(m+1)}\right) \\
&\quad + \epsilon\bar{P}(y) + \epsilon^2 p_2(x, y, t, \epsilon t) \\
u_{BC} &= \epsilon\frac{A(x - c_m t, \epsilon t)}{\sqrt{2}}\left(D_{m-1} - \frac{D_{m+1}}{(m+1)}\right) + \epsilon\bar{U}(y) + \epsilon^2 u_2(x, y, t, \epsilon t) \\
v_{BC} &= -\epsilon\left(\frac{2}{2m+1}\right)\frac{\partial A(x - c_m t, \epsilon t)}{\partial x}D_m + \epsilon^2 v_2(x, y, t, \epsilon t)
\end{aligned} \tag{18}$$

where l and c_m satisfy the resonance condition in (15) and the m subscripts have been omitted without ambiguity and for ease of notation. Note that the waves of different underlying wave speed from c_m will not be in resonance and are thus not included in the ansatz in (18).

In the model derived below the zonal means of the baroclinic and barotropic waves will be preserved by the dynamics. Therefore, without loss of generality, we require the zonal mean of the amplitudes A, B^S and B^A to vanish so that the zonal mean wind and vertical shear are completely specified by $\bar{\psi}$ and $\bar{U}$. This departure from the derivation of the amplitude equations in Majda and Biello [1] allows a more general meridional shear flow and serves to better distinguish the roles of meridionally symmetric and antisymmetric shears. In particular, the novel effects in the nonlinear theory arise when $\bar{U}$ has the opposite symmetry of the zonal component of the baroclinic wave. Henceforth we shall require $\bar{A} \equiv \int A(x, \epsilon t)\,dx = \bar{B}^S = \bar{B}^A = 0$, and denote the velocities associated with $\bar{U}$ and $\bar{\psi}$ as the zonal mean shear or wind.

To have weak dispersive effects compete with nonlinearity in these long-wave solutions (as in Refs. [1, 18, 19]) the zonal long-wave parameter δ in (10) and (11) and the amplitude, ϵ, in (18) are balanced and satisfy $\delta^2 = \epsilon$. As discussed in detail in Ref. [1] and Section 3.1, the reasonable value of $\epsilon = 0.1$ allows zonal velocities of order 5 ms^{-1} and, with $\delta^2 = \epsilon$, zonal variation on scales of order 5000 km; thus the relation $\delta^2 = \epsilon$ is physically realistic.

Solvability conditions to second order in ϵ for the expansion in (18) with this relationship of δ to ϵ yield the following *reduced equations for equatorial baroclinic-symmetric/antisymmetric barotropic waves* (BSAB)

$$\begin{aligned}
0 &= r_A A_\tau - D_A A_{xxx} + \mu A_x + \Gamma_S B^S_x + \Gamma_A B^A_x + \alpha(AB^S)_x \\
0 &= r_B B^S_\tau - D_B B^S_{xxx} + \Gamma_S A_x + \lambda B^S_x + \sigma B^A_x + \alpha A A_x \\
0 &= r_B B^A_\tau - D_B B^A_{xxx} + \Gamma_A A_x + \sigma B^S_x - \lambda B^A_x.
\end{aligned} \tag{19}$$

The detailed derivation will be presented in Section 3.1. Looking at (18) one sees that the BSAB equations describe a dispersive baroclinic wave, A, interacting with two dispersive barotropic waves, B^S and B^A, on timescales, $\tau = \epsilon t$, which are slow compared to the equatorial eddy turn-over time, T, from Equation (8). Nonlinear coupling occurs through the baroclinic and symmetric barotropic waves. The presence of a barotropic mean wind modifies the wave speeds through μ and λ and allows energy exchange among the barotropic waves through the nonzero coefficients σ. Baroclinic shear allows linear energy exchange between baroclinic and barotropic waves through $\Gamma_{A,S}$. The coefficients r_A, r_B, α and D_A, D_B, common to Ref. [1], are simply integrals of eigenfunctions and dispersions of the two sets of waves. The coefficients μ, λ, and σ are projections of functions of the mean wind, $\bar{\psi}$, onto the eigenfunctions of the waves. Lastly, $\Gamma_{A,S}$ are projections of functions of the mean baroclinic shear, defined by $\bar{U}(y)$, onto products of the wave eigenfunctions. It will be shown below that Γ_A (respectively Γ_S) vanishes if the baroclinic mean shear, $\bar{U}(y)$, has the same (opposite) meridional symmetry of the baroclinic waves under consideration.

3.1. Derivation of the BSAB equations

The asymptotic expansion from (18) is inserted into the LWSEBB equations in (10), (11) with $\delta^2 = \epsilon$ and successive powers of ϵ are required to vanish without secular behavior in time. As a consequence of the linear wave properties in (12) and (13) the terms of order ϵ automatically vanish. To consider the terms of order ϵ^2, the Riemann invariants, q and r, given in terms of p_{BC}, u_{BC} by $q = \frac{u+p}{\sqrt{2}}, r = \frac{u-p}{\sqrt{2}}$ are introduced [1, 16, 20]. The expansion of the baroclinic wave dynamics in (10) with (18) and $\delta^2 = \epsilon$ yields the following equations at order ϵ^2

$$
\begin{aligned}
q_{2,t} + q_{2,x} + L_- v_2 &= -q_{1,\tau} - (\psi_{1,x}(q_{1,y} + \bar{Q}_y) - (\psi_{1,y} + \bar{\psi}_y)q_{1,x}) \\
&\quad + \frac{1}{\sqrt{2}}\left[\left(\frac{q_1 + r_1}{\sqrt{2}} + \bar{U}\right)\psi_{1,xy} + v_1(\psi_{1,yy} + \bar{\psi}_{yy})\right] \\
r_{2,t} - r_{2,x} - L_+ v_2 &= -r_{1,\tau} - (\psi_{1,x}(r_{1,y} + \bar{R}_y) - (\psi_{1,y} + \bar{\psi}_y)r_{1,x}) \\
&\quad + \frac{1}{\sqrt{2}}\left[\left(\frac{q_1 + r_1}{\sqrt{2}} + \bar{U}\right)\psi_{1,xy} + v_1(\psi_{1,yy} + \bar{\psi}_{yy})\right] \\
L_+ q_2 - L_- r_2 &= c_m v_{1,x}
\end{aligned}
\tag{20}
$$

with $L_\pm$ the raising and lowering operators, $L_\pm = \frac{1}{\sqrt{2}}(\frac{d}{dy} \pm y)$

$$
\psi_1 = -B^S(x - c_m t, \tau)\sin(ly) - B^A(x - c_m t, \tau)\cos(ly) \tag{21}
$$

and q_1, r_1 calculated from the leading order baroclinic wave terms in (18). The functions $\bar{Q}(y)$ and $\bar{R}(y)$ are calculated from the baroclinic shear and pressure terms, $\bar{U}$ and $\bar{P}$ and, using (17), are related through

$$L_+\bar{Q} - L_-\bar{R} = 0. \tag{22}$$

Because we are considering traveling waves the substitution $v_{1,t}(x - c_m t, \epsilon t) = -c_m v_{1,x}(x - c_m t, \epsilon t)$, $c_m < 0$ has been used in the third equation in (20).

Recall that the amplitudes of the first order barotropic and baroclinic modes are waves traveling at the same speed so they will resonate with the linear waves at second order and generate secular terms. Such secular terms arise from the forcing functions on the right hand side of (20) which generate an amplitude response of order $\epsilon^2 t = \epsilon\tau$ that would be the same strength as the leading order terms in the analysis. On the other hand, the goal is to incorporate all of the nonlinear dynamics to the leading order self-consistently in the first order terms [1, 17, 20]. Thus the secular terms are required to vanish by requiring that the projection of the equations in (20) onto the eigenfunctions of the adjoint linear problem defined by the left hand side of (20) vanish. Because the linear operator is skew self-adjoint, the adjoint eigenfunction is equal to the eigenfunction itself. Therefore the integral over the domain of the inner product of the equations in (20) with

$$\begin{pmatrix} -\frac{1}{(m+1)} D_{m+1}(y)\phi(x) \\ D_{m-1}(y)\phi(x) \\ -\left(\frac{2}{2m+1}\right) D_m(y)\frac{\partial}{\partial x}\phi(x) \end{pmatrix} \equiv \begin{pmatrix} \hat{q}(y)\phi(x) \\ \hat{r}(y)\phi(x) \\ \hat{v}(y)\frac{\partial}{\partial x}\phi(x) \end{pmatrix} \tag{23}$$

must vanish for arbitrary $\phi(x)$; this relation also defines the eigenfunctions $\hat{q}(y), \hat{r}(y), \hat{v}(y)$. On performing this multiplication and integrating by parts to remove derivatives on $\phi(x)$, the first asymptotic equation in (19) emerges with explicit coefficients r_A, D_A, α, μ, Γ_S, Γ_A given by

$$\begin{aligned}
r_A &= \int_{-\infty}^{\infty} \left(\hat{q}^2 + \hat{r}^2\right) dy, \qquad D_A = \frac{1}{2m+1}\int_{-\infty}^{\infty} \hat{v}^2\, dy \\
\alpha &= -\int_{-\infty}^{\infty} \left[l^2 \sin(ly)\frac{\hat{v}}{\sqrt{2}}(\hat{q} + \hat{r}) - l\cos(ly)(\hat{q}^2 + \hat{r}^2)\right] dy \\
\Gamma_S &= -\int_{-\infty}^{\infty} \sin(ly)\left[\left(\frac{\hat{q} + \hat{r}}{\sqrt{2}}\bar{U}\right)_y + \hat{q}\,\bar{Q}_y + \hat{r}\,\bar{R}_y\right] dy \\
\Gamma_A &= -\int_{-\infty}^{\infty} \cos(ly)\left[\left(\frac{\hat{q} + \hat{r}}{\sqrt{2}}\bar{U}\right)_y + \hat{q}\,\bar{Q}_y + \hat{r}\,\bar{R}_y\right] dy \\
\mu &= \int_{-\infty}^{\infty} (\bar{\psi}_y + \bar{U}_{BT})\left[\left(\hat{v}\frac{\hat{q} + \hat{r}}{\sqrt{2}}\right)_y - (\hat{q}^2 + \hat{r}^2)\right] dy
\end{aligned} \tag{24}$$

where $\bar{U}_{BT}$ is the meridional average of the barotropic wind

$$\bar{U}_{BT} = \frac{1}{L}\int_{-\frac{L}{2}}^{\frac{L}{2}} -\bar{\psi}_y \, dy. \tag{25}$$

The definition of the barotropic mean advection, μ, contains the zonal mean barotropic velocity minus the meridional average of this mean wind and it will be convenient to define, $\bar{\psi}'_y \equiv \bar{\psi}_y + \bar{U}_{BT}$. This amounts to a Galilean transformation to the reference frame moving with the meridionally averaged barotropic wind; the same transformation will be made for the barotropic waves below. Because the original amplitudes were referred to a frame of reference moving with the baroclinic long wave speed, $-16.7\ \mathrm{m\,s^{-1}}$ for a dry atmosphere, this Galilean transformation refers the wave to a frame traveling with respect to the Earth's surface at the sum of the domain-averaged barotropic speed, $\epsilon\bar{U}_{BT}$ and the baroclinic long wave speed, c_m. Though this second transformation is not necessary, it serves to reduce the number of independent coefficients appearing in (19). Because the symmetry of $\hat{v}$ is always opposite the symmetry of $\hat{q}$ and $\hat{r}$, from the definition of μ in (24) we can see that only the symmetric component of the barotropic mean wind ($\bar{\psi}'$ antisymmetric) contributes to μ.

The other coefficients, r_A, D_A and α were already presented in Ref. [1]. It was discussed in Ref. [1] that the coefficients of $A_x B^S$ and AB_x^S were numerically determined to always be equal and equal to α; a necessary condition for the baroclinic zonal mean, $\bar{A}$, to be conserved. A straightforward analytic proof of this fact follows the proof in Appendix A of the equivalence of the coefficients Γ_A appearing in the baroclinic and barotropic wave equations.

The terms proportional to Γ_A and Γ_S linearly couple baroclinic and barotropic waves. In these integrals the zonal velocity associated with the baroclinic meridional eigenfunctions, $\hat{q}, \hat{r}$ is $\hat{u} = \frac{\hat{q}+\hat{r}}{\sqrt{2}}$, thus $\hat{u}$, $\hat{q}$, and $\hat{r}$ have the same meridional symmetry as do $\bar{U}$, $\bar{Q}$, and $\bar{R}$. Therefore only the component of the baroclinic shear, $\bar{U}$, with the *same* symmetry as the baroclinic wave, $\hat{u}$, contributes to the coupling coefficient of the baroclinic wave to a symmetric barotropic wave, Γ_S. Similarly, only the component of the baroclinic shear, $\bar{U}$, with the *opposite* symmetry as the baroclinic wave, $\hat{u}$, contributes to the coupling coefficient of the baroclinic wave to an antisymmetric barotropic wave, Γ_A.

The derivation of the two barotropic wave equations proceeds in a similar fashion. Using (18) in (11) and $\delta^2 = \epsilon$ the first order terms are satisfied by construction. At second order we find

$$\begin{aligned}
\psi_{2yyt} + \psi_{2x} &= -\big(\psi_{1,yy\tau} + \psi_{1,x}(\psi_{1,yyy} + \bar{\psi}_{yyy}) - (\psi_{1,y} + \bar{\psi}_y)\psi_{1,xyy} \\
&\quad - \big(u_1^2\big)_{xy} - (u_1 v_1)_{yy} - 2(\bar{U}u_1)_{xy} - (\bar{U}v_1)_{yy} + \psi_{1,xxt}\big) \\
&= -\big(\psi_{1,yy\tau} + \psi_{1,xxt} + \psi_{1,x}\bar{\psi}_{yyy} - \bar{\psi}_y\psi_{1,xyy} \\
&\quad - \big(u_1^2\big)_{xy} - (u_1 v_1)_{yy} - 2(\bar{U}u_1)_{xy} - (\bar{U}v_1)_{yy}\big)
\end{aligned} \tag{26}$$

where again ψ_1 is given by (21) and u_1, v_1 are the leading-order baroclinic wave components from (18). Because $\psi_{1,yy} \propto \psi_1$ the wave self-advection terms vanish, giving rise to the second equality. Again the terms on the right hand side would produce secular growth of ψ_2 and must be removed; this is achieved by multiplying the left hand side by each of the functions $\sin(ly)$, $\cos(ly)$ and integrating from $-L/2 \le y \le L/2$. We again consider baroclinic zonal shears $\bar{U}$ and will make the Galilean transformation to the frame of reference moving with the mean barotropic wind speed, $\epsilon \bar{U}_{BT}$, so that the last two equations in (19) emerge with coefficients

$$
\begin{aligned}
r_B &= l^2 \frac{L}{2}, \qquad D_B = \frac{1}{l^2}\frac{L}{2} \\
\alpha &= \int_{-\infty}^{\infty} \left[l \cos(ly)(\hat{q}+\hat{r})^2 + l^2 \sin(ly) \frac{\hat{v}}{\sqrt{2}}(\hat{q}+\hat{r}) \right] dy \\
\Gamma_S &= \int_{-\infty}^{\infty} \left[\sqrt{2} l \cos(ly)(\hat{q}+\hat{r})\bar{U} + l^2 \sin(ly)\hat{v}\bar{U} \right] dy \\
\Gamma_A &= \int_{-\infty}^{\infty} \left[-\sqrt{2} l \sin(ly)(\hat{q}+\hat{r})\bar{U} + l^2 \cos(ly)\hat{v}\bar{U} \right] dy \\
\lambda &= -\int_{-\frac{L}{2}}^{\frac{L}{2}} \sin^2(ly)(\bar{\psi}'_{yyy} + l^2 \bar{\psi}'_y)\, dy = -\frac{3}{2}\int_{-\frac{L}{2}}^{\frac{L}{2}} l^2 \cos(2ly)\bar{\psi}'_y\, dy \\
\sigma &= -\int_{-\frac{L}{2}}^{\frac{L}{2}} \sin(ly)\cos(ly)(\bar{\psi}'_{yyy} + l^2 \bar{\psi}'_y)\, dy = \frac{3}{2}\int_{-\frac{L}{2}}^{\frac{L}{2}} l^2 \sin(2ly)\bar{\psi}'_y\, dy
\end{aligned}
\tag{27}
$$

where integration by parts has been performed on the relations defining λ and σ. Strictly speaking we have taken the domain of integration to infinity for the baroclinic coupling coefficients. It was argued in Ref. [1] that because the baroclinic eigenfunctions decay exponentially away from the origin and if we assume that $\bar{U}$ is well behaved, then the equations incur only exponentially small errors with this simplification. Furthermore, having again transformed to a reference frame moving at the domain averaged barotropic velocity, $\epsilon \bar{U}_{BT}$, the deviation from this mean, $\bar{\psi}'_y$, appears in the definition of the barotropic advection coefficients λ, σ.

The coefficients have some interesting properties that merit emphasis. There are terms which vanish identically due to symmetry considerations and have not been shown. For example, there is no nonlinear AA_x term in the evolution equation for B^A in (19). In Appendix A we provide the proof that for arbitrary velocities, $\bar{U}$, Γ_A in (24) is equal to its counterpart in (27); the corresponding proofs for Γ_S and α follow the same steps and are omitted. This equality is necessary in order that the amplitude equations conserve energy. In the definition of λ note that only symmetric zonal velocities ($\bar{\psi}$ antisymmetric) contribute; so, too, in the definition of σ only antisymmetric zonal velocities

($\bar{\psi}$ symmetric) contribute. Lastly note that if $\bar{\psi}$ is a solution of $\bar{\psi}_{yy} + l^2\bar{\psi} = 0$, that is, if it has the same meridional wavenumber as the barotropic wave, then it does not provide any additional advection to the barotropic waves, as is required for self-consistency.

In summary, the BSAB Equations (19) describe the interaction of weakly dispersive equatorial baroclinic Rossby waves, A, with symmetric and antisymmetric barotropic Rossby waves having a significant midlatitude projection, B^S, B^A. The waves are referred to the reference frame traveling at the sum of the long Rossby wave speed (-16.7 m/s) corrected by the domain-averaged wind, $\epsilon\bar{U}_{BT}$ with $\bar{U}_{BT} \equiv -\frac{1}{L}\int_{-L/2}^{L/2} \bar{\psi}_y\, dy$. There is relative dispersion of the barotropic and baroclinic waves accounted for in the third derivative terms. Their interaction is facilitated by the presence of zonal mean wind and shear, $\bar{\psi}, \bar{U}^S$ through the linear terms in (19). Baroclinic waves are coupled to meridionally symmetric barotropic waves in the presence of a baroclinic mean shear of the same meridional symmetry of the baroclinic wave. Conversely, baroclinic waves are coupled to antisymmetric barotropic waves in the presence of a baroclinic mean shear of the opposite symmetry of the baroclinic wave. A symmetric mean barotropic wind advects the baroclinic wave (μ) and splits the wave speeds of the symmetric and antisymmetric barotropic waves (λ). An antisymmetric mean barotropic wind couples the symmetric and antisymmetric barotropic waves (σ). Nonlinear coupling enters only through wave–wave interaction of baroclinic waves and symmetric barotropic waves, AB_x^S, AA_x. These effects will be elaborated upon below.

4. Properties of the BSAB equations

Upon rescaling the zonal coordinate, time, and the wave amplitudes in (19) we arrive at the canonical form of the BSAB equations

$$\begin{aligned} 0 &= A_\tau - DA_{xxx} + \mu A_x + \Gamma_S B_x^S + \Gamma_A B_x^A + (AB^S)_x \\ 0 &= B_\tau^S - B_{xxx}^S + \Gamma_S A_x + \lambda B_x^S + \sigma B_x^A + AA_x \\ 0 &= B_\tau^A - B_{xxx}^A + \Gamma_A A_x + \sigma B_x^S - \lambda B_x^A \end{aligned} \tag{28}$$

where the amplitudes, x, τ, and all parameters other than D are given the same notation as in (19). This is the same rescaling derived in Ref. [1] and the parameters of the rescaling are presented in Appendix B. The only remaining parameter which does not depend on the shears is the ratio of dispersions, D, which is given by

$$D = 1 - \frac{1}{(2m+1)^2}. \tag{29}$$

For the examples we shall solely be interested in $m = 1, 2$, the first symmetric and antisymmetric baroclinic waves. These are the only baroclinic waves whose

meridional extent is physically compatible with the β-plane approximation. The specific values of the other parameters are given by the components of the shear and wind and will be presented when examples are discussed below.

4.1. Conserved quantities and Hamiltonian structure

Because the equations in (28) are in gradient form it is clear that the zonal means $\bar{A} \equiv \int A(x,\tau)\,dx$, $\bar{B}^S$ and $\bar{B}^A$ are constant in time and so, too, their corresponding zonal shear and winds are constant. Total zonal winds and shears for the examples considered below are shown in Figures 1, 5, 9, and 13 and have typical features and strengths of tropical shears.

Furthermore a straightforward calculation shows that the total energy

$$E = \int \left[A^2 + (B^S)^2 + (B^A)^2\right] dx \tag{30}$$

is conserved. The energy in the individual waves is

$$E_A = \int \frac{(A)^2}{2} dx, \quad E_{B^S} = \int \frac{(B^S)^2}{2}\, dx, \quad E_{B^A} = \int \frac{(B^A)^2}{2}\, dx \tag{31}$$

and some straightforward manipulations of (28) yield the energy exchanges

$$\begin{aligned}
\frac{dE_A}{dt} &= -\frac{\Gamma_S}{2}\int \left(AB_x^S - B^S A_x\right) dx - \frac{\Gamma_A}{2}\int \left(AB_x^A - B^A A_x\right) dx \\
&\quad - \frac{1}{2}\int (A)^2 B_x^S\, dx \\
\frac{dE_{B^S}}{dt} &= \frac{\Gamma_S}{2}\int \left(AB_x^S - B^S A_x\right) dx - \frac{\sigma}{2}\int \left(B^S B_x^A - B^A B_x^S\right) dx \\
&\quad + \frac{1}{2}\int (A)^2 B_x^S\, dx \\
\frac{dE_{B^A}}{dt} &= \frac{\Gamma_A}{2}\int \left(AB_x^A - B^A A_x\right) dx + \frac{\sigma}{2}\int \left(B^S B_x^A - B^A B_x^S\right) dx.
\end{aligned} \tag{32}$$

This form of the energy budget makes transparent the principles stated above that baroclinic mean shear of the same symmetry of the baroclinic waves couples these waves to symmetric barotropic waves (Γ_S terms). Conversely baroclinic mean shear of the opposite symmetry of the baroclinic waves (Γ_A terms) couples baroclinic waves to antisymmetric barotropic waves. Furthermore the only nonlinear energy transfer couples baroclinic waves to symmetric barotropic waves (the cubic term) and there is a route for energy exchange from symmetric to antisymmetric barotropic waves through antisymmetric barotropic winds (σ terms).

By the resonance condition (15) it is clear that the waves described by (28) do not interact with any equatorial waves traveling at a different carrier

velocity, c_m. Because the zonal means are conserved the baroclinic waves of different meridional symmetry do not interact with one another. However, on the time and length scales appropriate to the BSAB equations the atmosphere is strongly affected by boundary layer drag, thermal dissipation, and forcing. Each of these mechanisms would break both energy and mean flow conservation creating the possibility for the interaction of waves of different carrier speeds, c_m. Such interactions are interesting but beyond the scope of the present work. The remarkable effects of equatorial boundary layer drag are presented in a companion paper of the authors [21].

The BSAB equations also have a Hamiltonian structure. Using the bracket

$$\{F, G\} = -\int \left[\frac{\delta F}{\delta A}\frac{\partial}{\partial x}\frac{\delta G}{\delta A} + \frac{\delta F}{\delta B^S}\frac{\partial}{\partial x}\frac{\delta G}{\delta B^S} + \frac{\delta F}{\delta B^A}\frac{\partial}{\partial x}\frac{\delta G}{\delta B^A} \right] dx \tag{33}$$

another straightforward calculation shows that the Hamiltonian,

$$\begin{aligned} H = \frac{1}{2}\int \Big[& DA_x^2 + \left(B_x^S\right)^2 + \left(B_x^A\right)^2 + A^2 B^S + \mu A^2 \\ & + 2A\left(\Gamma_S B^S + \Gamma_A B^A\right) + \lambda\left((B^S)^2 - (B^A)^2\right) + 2\sigma B^A B^S \Big] dx \end{aligned} \tag{34}$$

generates the dynamics of (28) through $A_\tau = \{A, H\}$, etc. and H is conserved. Lastly note that when Γ_A, λ, and σ vanish Equations (28) reduce to the amplitude equations presented in Ref. [1] plus a trivial linear dispersion equation for B^A. The implications for the mean wind and shear will become clear below.

4.2. Normal form of the amplitude equations

The barotropic components of the amplitude equations have a term proportional to

$$M \equiv \begin{bmatrix} \lambda & \sigma \\ \sigma & -\lambda \end{bmatrix} \tag{35}$$

which can clearly be diagonalized with a rotation matrix $\mathbf{R}(\theta)$. Defining

$$\begin{bmatrix} B^E \\ B^W \end{bmatrix} = \begin{bmatrix} \cos(\theta) & \sin(\theta) \\ -\sin(\theta) & \cos(\theta) \end{bmatrix} \begin{bmatrix} B^S \\ B^A \end{bmatrix} \tag{36}$$

and conjugating M with $\mathbf{R}$ we find

$$N \equiv \mathbf{R}M\mathbf{R}^T = \begin{bmatrix} V & 0 \\ 0 & -V \end{bmatrix} \tag{37}$$

where

$$V = \sqrt{\lambda^2 + \sigma^2} \quad \text{and} \quad \tan(2\theta) = \frac{\sigma}{\lambda}. \tag{38}$$

Rewriting the amplitude equations in terms of the new variables B^E, B^W yields the normal form for equatorial baroclinic/barotropic waves (NFEBBW)

$$\begin{aligned} A_\tau - DA_{xxx} + \mu A_x + \Gamma_E B^E_x + \Gamma_W B^W_x + [A(B^E\cos(\theta) - B^W\sin(\theta))]_x = 0 \\ B^E_\tau - B^E_{xxx} + V B^E_x + \Gamma_E A_x + A_x A\cos(\theta) = 0 \\ B^W_\tau - B^W_{xxx} - V B^W_x + \Gamma_W A_x - A_x A\sin(\theta) = 0 \end{aligned} \tag{39}$$

The baroclinic coupling terms become

$$\begin{aligned} \Gamma_E &= \Gamma_S\cos(\theta) + \Gamma_A\sin(\theta) \\ \Gamma_W &= -\Gamma_S\sin(\theta) + \Gamma_A\cos(\theta). \end{aligned} \tag{40}$$

In the limit of linear long waves and in a frame of reference moving with the sum of the Rossby wave speed and mean barotropic velocity (as discussed above) when there is no baroclinic shear the barotropic waves split into an eastward traveling wave, B^E, and a westward traveling wave, B^W, each with velocity V due to the barotropic shear. The barotropic shear continues to impart a velocity, μ, to the baroclinic waves.

4.3. Interpretation of the normal form parameters

To interpret the parameters of the normal form it is convenient to pick an example with a specific barotropic mean wind. Consider a barotropic zonal wind with a Gaussian profile centered about a latitude y_*

$$U_{BT} = -\bar{\psi}_y = U_* e^{-\frac{(y-y_*)^2}{2\sigma^2}}. \tag{41}$$

Substituting the expressions in (27), integrated over an infinite domain (and incurring an exponentially small error as already discussed), into (38) yields

$$\tan(2\theta) = \frac{\sigma}{\lambda} = \frac{-\int_{-\infty}^{\infty}\sin(2ly)\bar{\psi}'_y\,dy}{\int_{-\infty}^{\infty}\cos(2ly)\bar{\psi}'_y\,dy}. \tag{42}$$

After a straightforward manipulation we find

$$\theta = -y_* l \tag{43}$$

and the barotropic advection velocity

$$V = \sqrt{\lambda^2 + \sigma^2} \propto U_*(\sigma l)e^{-2(\sigma l)^2} \tag{44}$$

where λ and η in these expressions are the rescaled coefficients, that is to say the corresponding coefficients from (24) divided by r_B.

The stream function associated with a pure B^E state has $B^W = 0 = -B^S \sin(\theta) + B^A \cos(\theta)$ and, therefore,

$$\begin{aligned}\psi^E &\propto -(B^S \sin(ly) + B^A \cos(ly)) \\ &\propto \sin(ly + \theta) = \sin(l(y - y_*)).\end{aligned} \tag{45}$$

Similarly the stream function associated with a pure B^W state has $B^E = 0 = B^S \cos(\theta) + B^A \sin(\theta)$ and therefore

$$\begin{aligned}\psi^W &\propto -(B^S \sin(ly) + B^A \cos(ly)) \\ &\propto \cos(ly + \theta) = \cos(l(y - y_*)).\end{aligned} \tag{46}$$

We can now interpret the terms in the normal form (39) given a barotropic wind as in (41) centered about a latitude y_* with maximum strength U_*. The first barotropic eigenfunction corresponds to waves B^E whose zonal velocity is symmetric about the latitude y_* (Equation (45)) and traveling *eastward* (relative to the moving frame) at a velocity proportional to U_* in the long wave limit. The second barotropic eigenfunction corresponds to waves B^W whose zonal velocity is antisymmetric about the latitude y_* (Equation (46)) and traveling *westward* at a velocity proportional to U_* in the long wave limit.

The linear terms which couple baroclinic and barotropic waves can be simplified using (24), (40), (43), and (B.3)

$$\begin{aligned}\Gamma_E &= -\frac{\sqrt{r_A}}{\alpha} \int_{-\infty}^{\infty} \sin(l(y - y_*)) \left[(\hat{u}\bar{U})_y + \hat{q}\,\bar{Q}_y + \hat{r}\,\bar{R}_y\right] dy \\ \Gamma_W &= -\frac{\sqrt{r_A}}{\alpha} \int_{-\infty}^{\infty} \cos(l(y - y_*)) \left[(\hat{u}\bar{U})_y + \hat{q}\,\bar{Q}_y + \hat{r}\,\bar{R}_y\right] dy\end{aligned} \tag{47}$$

and are identical to the definitions of Γ_S, Γ_A except projected around the origin of the new barotropic waves, y_*. Therefore, in the sense of linear theory, y_* amounts to a shift of origin of the waves to the midpoint of the barotropic wind. In fact, the linear terms in (39) have the same structure, albeit with different parameters, as the linear terms in (28) with the antisymmetric barotropic shear set to zero.

The normal form (39) comes at the expense of adding two nonlinear terms, but they are readily interpreted as follows. Writing the barotropic stream function

$$\psi = -B^E \sin(l(y - y_*)) - B^W \cos(l(y - y_*))$$

its corresponding zonal velocity

$$u_{BT} = -\psi_y = l\big(B^E \cos(l(y - y_*)) - B^W \sin(l(y - y_*))\big).$$

Evaluating the zonal velocity at $y = 0$ results in

$$u_{BT}(x, 0, \tau) = l\left(B^E \cos(ly_*) + B^W \sin(ly_*)\right)$$
$$= l(B^E \cos(\theta) - B^W \sin(\theta)). \tag{48}$$

Comparing with the normal form equations (39) it is clear that the nonlinear baroclinic coupling to each barotropic wave is proportional to the zonal velocity of that wave evaluated at $y = 0$. This is not surprising because the meridional structure of the baroclinic waves is strongly concentrated near the origin. In conclusion baroclinic waves are generated by the zonal component of the barotropic wave at the equator.

The example barotropic shear is quite specific and was chosen because the coefficients are analytically calculable. Another useful example is a model wind, which is antisymmetric about a latitude y_*; the derivative of the Gaussian in (41) shall suffice. In this case, a straightforward calculation yields

$$\theta = -ly_* + \frac{\pi}{4}. \tag{49}$$

The meridional eigenfunctions have zonal velocity which is maximum at $y = y_* \pm \frac{\pi}{4l}$ and zero at $y = y_* \mp \frac{\pi}{4l}$, respectively. The same eigenvalues, interpretation of baroclinic coupling, and interpretation of nonlinear terms holds as for the previous example.

In the case with no barotropic wind the only remaining parameters are the Γ's, which linearly couple baroclinic to barotropic waves. In this case there exists another rotation of the barotropic block, which removes one of these coupling terms. The Equation (39) results with the barotropic advection parameters, μ and V equal to zero; the physical meaning of this rotation in terms of the mean baroclinic shear is not as straightforward to decipher. However the rotation itself again amounts to a meridional displacement of the latitude of symmetry of the waves so that the baroclinic waves linearly drive only the barotropic waves, which are symmetric about that latitude.

5. Nonlinear dynamics of the BSAB equations

Having described the physical intuition we can proceed to study both numerical and, in the subsequent section, analytical solutions to the Equations (28) in physically relevant parameter regimes. Here we focus on the new effects of antisymmetric mean shear on $m = 1$ baroclinic waves and $l = \sqrt{3}$ barotropic waves.

We begin by studying the exchange of energy from barotropic waves to baroclinic waves using a variant of the example described by Majda and Biello in Ref. [1] with the addition of antisymmetric baroclinic shear. In that example it was shown that barotropic waves drive equatorially confined $m = 1$ baroclinic waves on timescales of less than 20 days. This remains true in

the presence of a moderate amount of antisymmetric baroclinic shear but by increasing the strength of the antisymmetric shear the antisymmetric barotropic waves are driven strongly enough to draw energy from the baroclinic waves.

The second example explores the combined effect of both an antisymmetric wind and shear in addition to symmetric components. The initial condition of random $m = 1$ baroclinic waves drives barotropic waves of both symmetries effectively fixing their relative amplitudes.

The third example explores the effect of a purely antisymmetric wind and shear on the transport of energy from antisymmetric barotropic waves to $m = 1$ baroclinic waves. Though less relevant from the perspective of the atmospheric sciences, this case yields intriguing asymmetric vortices and dramatically tilted shears.

Numerical integrations were performed using a de-aliased pseudo-spectral method with 64 modes of spatial resolution combined with a fourth order Runge-Kutta time discretization. Conservation of energy to within 10^{-6} is satisfied for all numerical solutions. To reconstruct the velocity fields the standard value of $c = 50$ ms^{-1} and the choice $\epsilon = 0.1$ is used. In all of the following numerical experiments the energy was initially supplied to the first four wave numbers with statistically identical random amplitudes and phases. The amplitudes were chosen so that the root mean square amplitudes did not exceed 5 ms^{-1} in order that they be compatible with the value $\epsilon = 0.1$. As in Ref. [1] to be consistent with $\delta = \sqrt{\epsilon} = 0.316$ only the first eight modes are valid for the asymptotics of $m = 1$; the integrations were monitored to ensure that less than 4% of the conserved total wave energy was present in wavenumbers higher than these thresholds. See Ref. [1] for a detailed description of these tests.

5.1. Antisymmetric shear modifying m = 1 energy transfer

The first example in Ref. [1] used a baroclinic mean shear, $\bar{A}$, corresponding to 5 ms^{-1} and no barotropic mean wind. The meridional structure of the baroclinic shear is exactly that of the $m = 1$ baroclinic wave. The initial condition consisted of a random seed of barotropic waves, which then developed mostly equatorial baroclinic wave energy on timescales of less than 20 days. In fact, the structure of the baroclinic waves was strongly localized and resembled a "westerly wind burst" with a strong cyclone pair at the bottom and strong anticyclone pair at the top of the troposphere. This example is repeated here with the addition of an antisymmetric baroclinic shear having the meridional structure of an $m = 2$ baroclinic wave and a velocity of 2.5 ms^{-1} at its maximum.

Figure 1 shows the mean velocities resulting from the baroclinic shear at the bottom, (a), and top, (b), of the troposphere. In fact the combination essentially amounts to a northward shift of the extrema of the baroclinic shear to about 500 km north of the equator (and remains top/bottom antisymmetric).

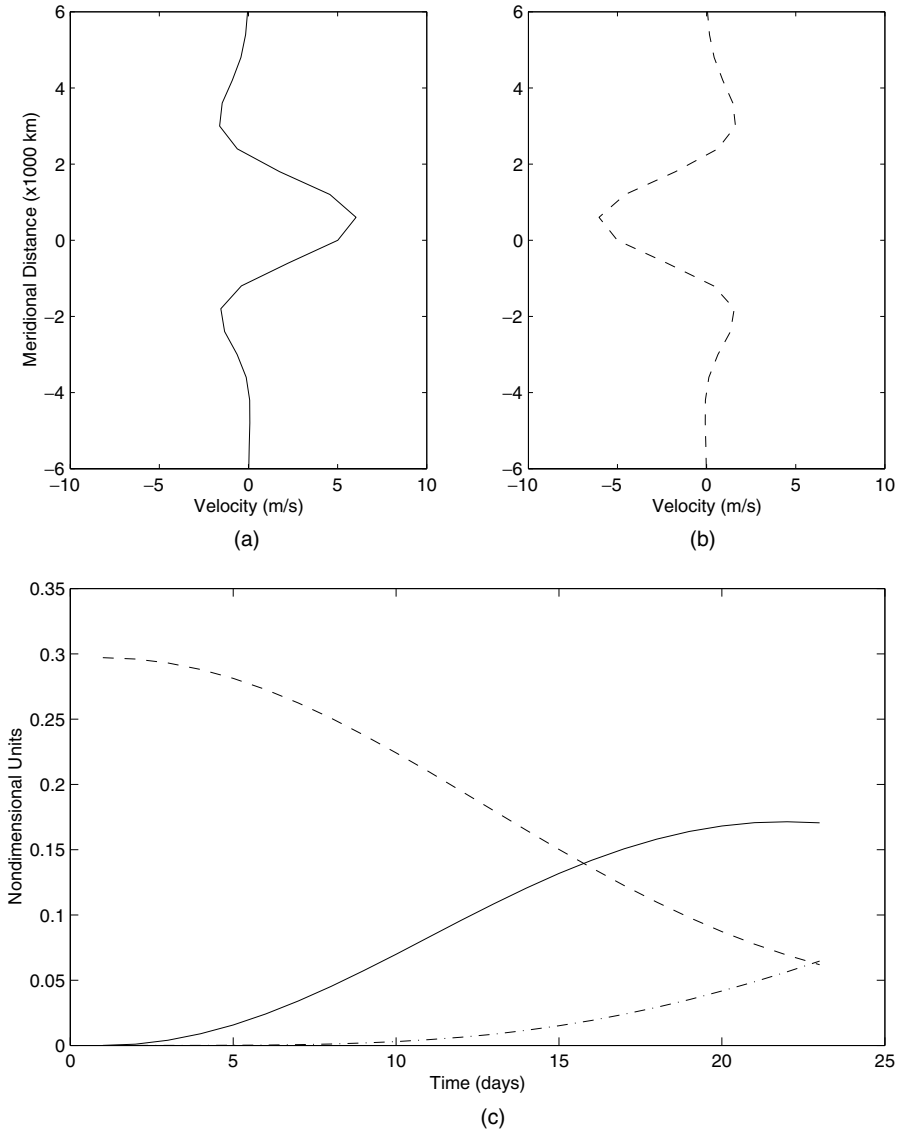

Figure 1. Zonal mean velocity (a) bottom and (b) top of troposphere for the first example of Section 5.1 with the addition of a 2.5 m s^{-1} antisymmetric baroclinic shear to a 5 m s^{-1} symmetric shear. (c) The energy in the symmetric barotropic (B^S, dash), symmetric baroclinic (A, solid) and antisymmetric barotropic waves (B^A, dot-dash) as a function of time.

Figure 1(c) indicates that a significant fraction of the wave energy is driven to the barotropic modes at 22 days with a nearly equal fraction in both the barotropic waves. Though energetically benign, the addition of antisymmetric shear has significant consequences on the velocity field. Figure 2 shows the

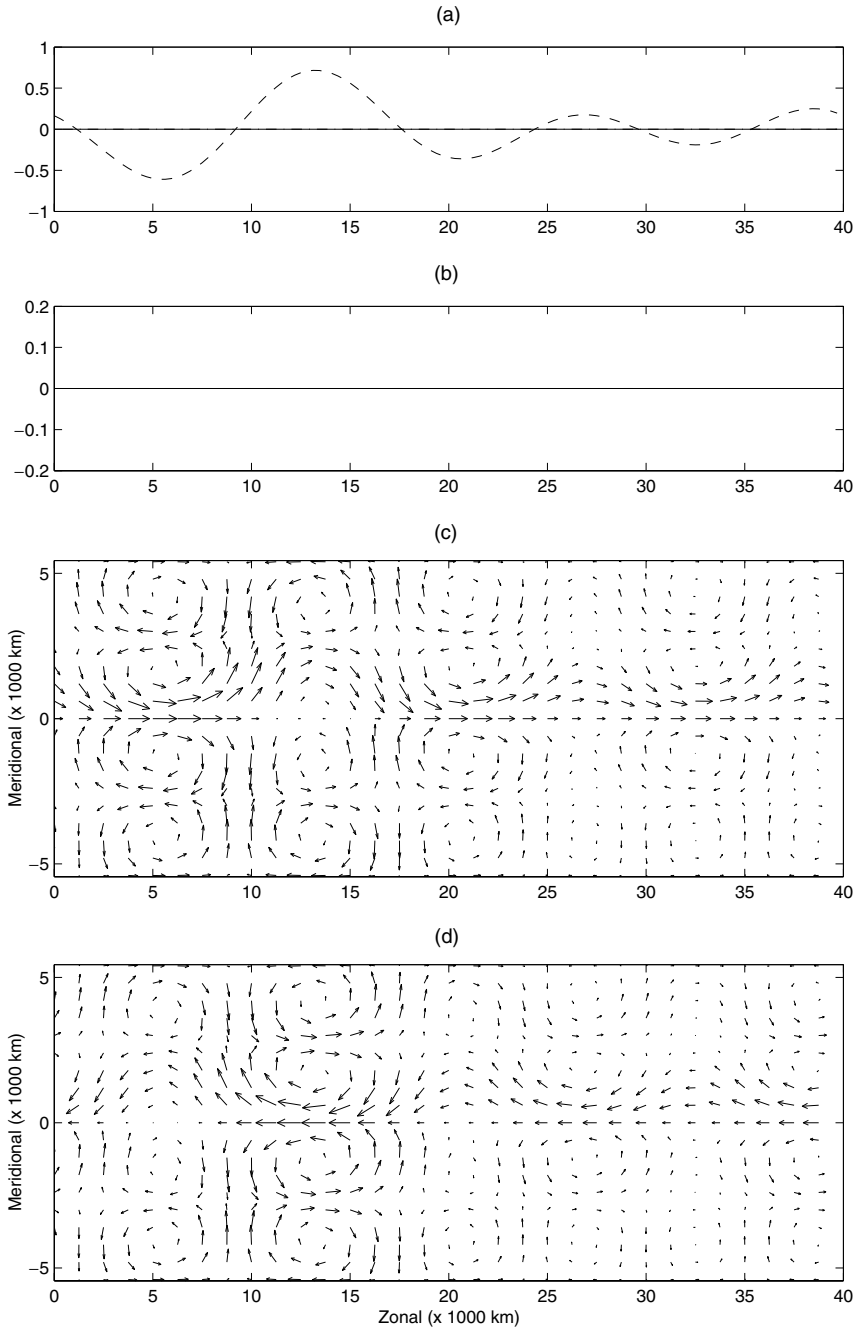

Figure 2. (a) Nondimensionalized wave amplitude, A, solid; B^S, dash; B^A, dot-dash. (b) Flux densities, $A - B^S$, dot-dash; $A - B^A$, dash; $B^S - B^A$, dot; nonlinear term, solid. (c) The total velocity at the top of the troposphere and (d) The total velocity at the bottom of the troposphere for the example shear from Figure 1 and Section 5.1 at time $t = 0$.

initial barotropic wave amplitude, energy flux (the terms in Equation (32)), and the corresponding velocity field at the top and bottom of the troposphere. The jet is centered at about 500 km north of the equator and the presence of the barotropic wave causes a marked meander at the bottom of the troposphere. At 12 days (Figure 3) a strong baroclinic wave dominates the flow in the form of a pair of anticyclonic waves leading a pair of cyclonic waves at the bottom of the troposphere near $x = 15$. The energy transfer is due mainly to the coupling of the symmetric barotropic wave to the baroclinic wave through the mean baroclinic shear and is also centered at $x = 15$. There is also a dipolar nonlinear energy exchange (solid curve), which tends to drive the barotropic wave energy on the western side of a barotropic cyclone and deplete it on the eastern side. The winds are reminiscent of a "westerly wind burst" as discussed in Ref. [1] with an important distinction. Even though there is, as of yet, only a weak antisymmetric barotropic wave, the fact that the mean baroclinic wave is not centered on the mean baroclinic shear gives a distinct northward tilt to the burst.

Figure 4 shows that at 20 days the baroclinic waves begin to significantly drive antisymmetric barotropic waves. The baroclinic component does not propagate beyond its original location whereas the nascent antisymmetric barotropic wave is as strong in places as the symmetric component. Two baroclinic bursts dominate at 20 days and the winds are clearly tilted northward. We conclude that the presence of a moderate antisymmetric baroclinic shear does not greatly affect the exchange of energy between barotropic an baroclinic waves. Although there is a marked northward tilt in the resulting winds, they are otherwise identical to the "westerly wind burst" phenomenon discussed in Ref. [1].

A strong antisymmetric baroclinic shear can, however, greatly influence this energy transfer as discussed next in the second example. Figure 5 shows the profile, top and bottom, of a purely baroclinic zonal mean shear. The lower figure indicates that a random initial barotropic wave train excites equatorial baroclinic waves but these baroclinic waves in turn excite antisymmetric barotropic waves. In fact, by 20 days the profile is dominated by the barotropic waves and remains so for a long time afterward. The shears are qualitatively the same as those in Figure 1 and differ only in that the maximum and minimum are of greater amplitude and occur slightly northward of their counterparts. The initial profile in Figure 6 also does not qualitatively differ from the previous example. Figure 7 shows that there is a significant difference both in the wave amplitudes and energy flux at 10 days. Though energy is being pumped into the baroclinic waves (dot-dash curve in Figure 7(b)) there is an opposing pump of energy from the baroclinic waves to the antisymmetric barotropic waves, which begins to dominate throughout the domain (dashed curve). In fact, by 20 days (Figure 8) baroclinic wave pumping of antisymmetric barotropic waves dominates throughout the domain. In fact the antisymmetric barotropic amplitude is about 1.5 times the symmetric barotropic amplitude through much of the domain. Using Equation (21) and (48) we see that such

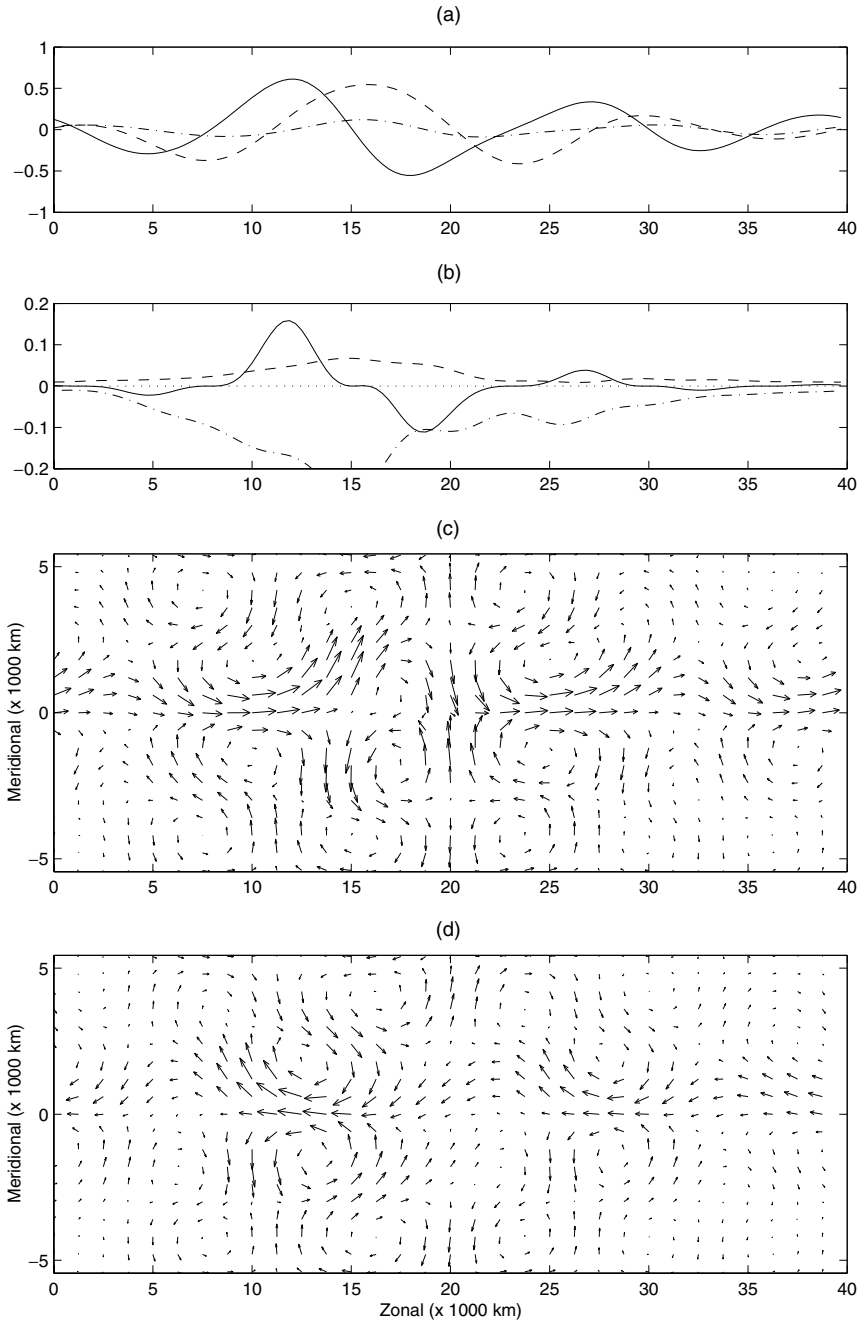

Figure 3. (a) Nondimensionalized wave amplitude, A, solid; B^S, dash; B^A, dot-dash. (b) Flux densities, $A - B^S$, dot-dash; $A - B^A$, dash; $B^S - B^A$, dot; nonlinear term, solid. (c) The total velocity at the top of the troposphere and (d) The total velocity at the bottom of the troposphere for the example shear from Figure 1 and Section 5.1 at a time of 12 days.

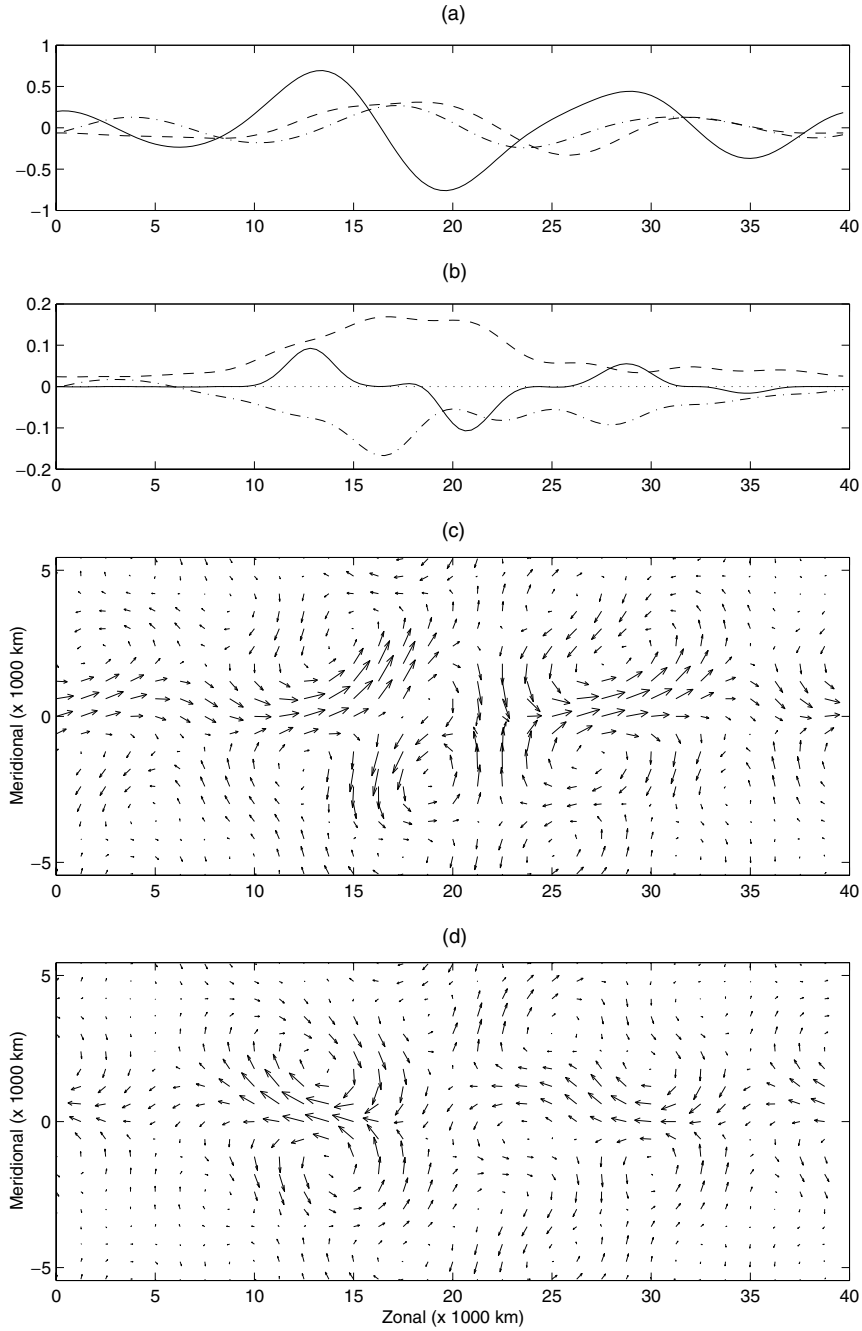

Figure 4. (a) Nondimensionalized wave amplitude, A, solid; B^S, dash; B^A, dot-dash. (b) Flux densities, $A - B^S$, dot-dash; $A - B^A$, dash; $B^S - B^A$, dot; nonlinear term, solid. (c) The total velocity at the top of the troposphere and (d) The total velocity at the bottom of the troposphere for the example shear from Figure 1 and Section 5.1 at a time of 20 days.

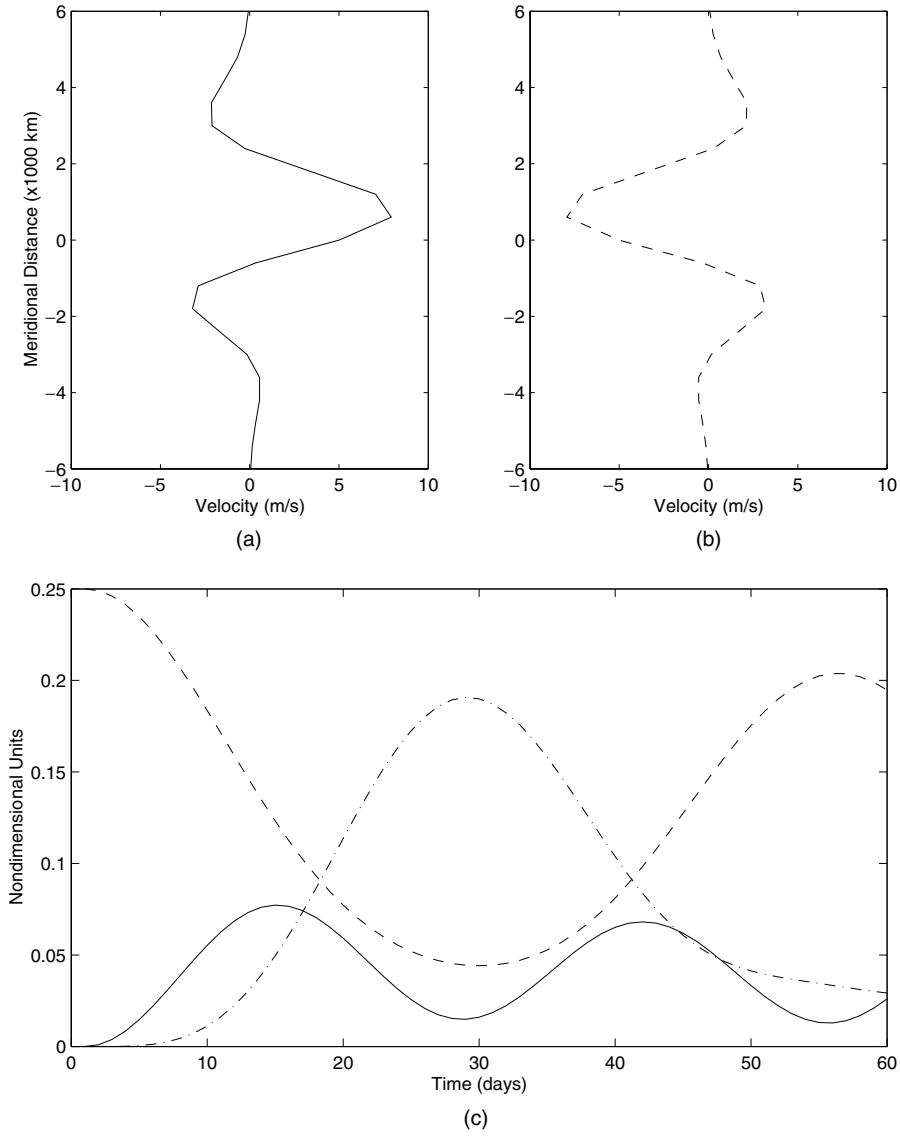

Figure 5. Zonal mean velocity (a) bottom and (b) top of troposphere for the second example of Section 5.1 with the addition of a 5 m s^{-1} antisymmetric baroclinic shear to a 5 m s^{-1} symmetric shear. (c) The energy in the symmetric barotropic (B^S, dash), symmetric baroclinic (A, solid) and antisymmetric barotropic waves (B^A, dot-dash) as a function of time.

waves are simply a barotropic wave train shifted northward by $y_* = (3\pi)/(4l)$, approximately 1800 km. This is reflected in Figure 8(c), where the velocity at the bottom of the troposphere shows three barotropic anticyclones at the crest of the baroclinic jet at about 2000 km north.

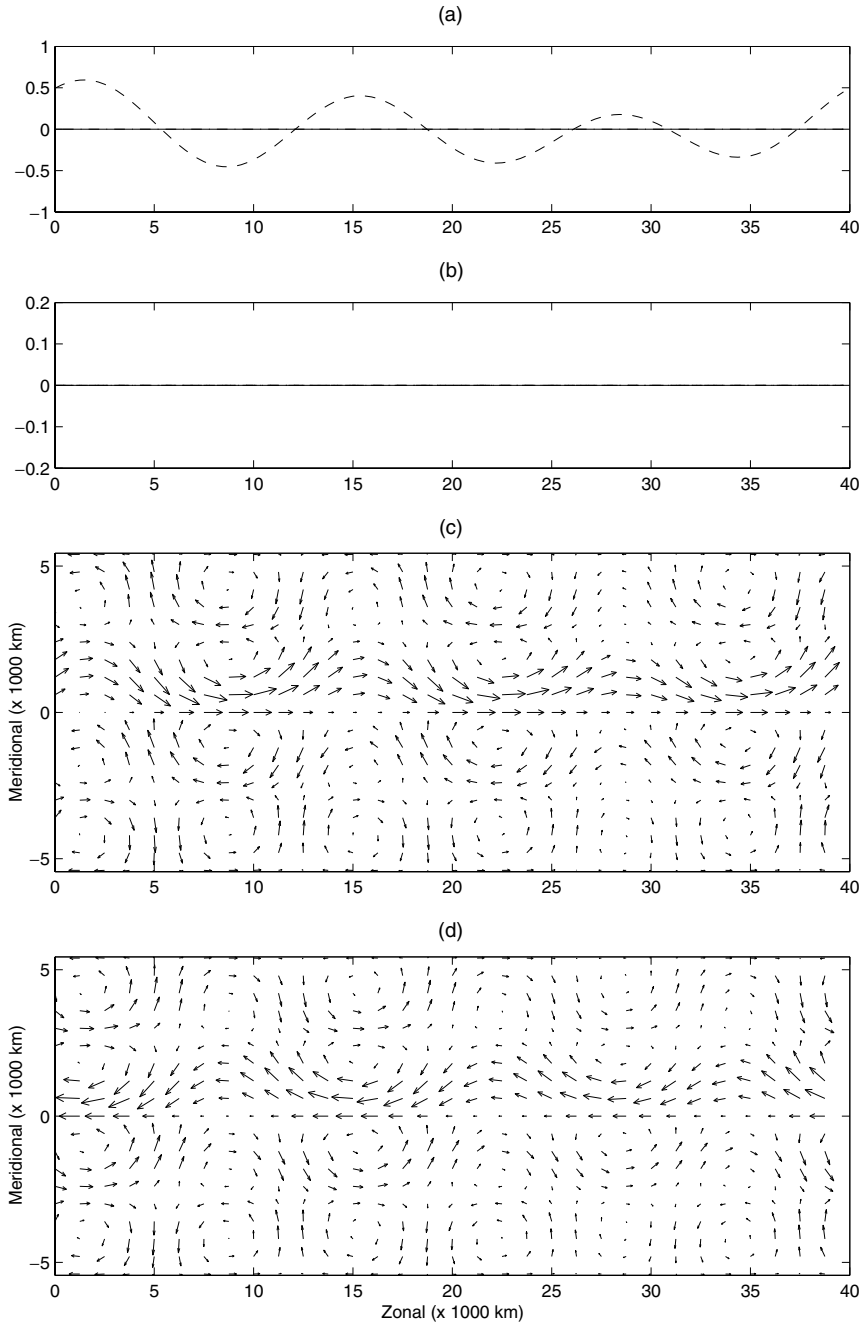

Figure 6. (a) Nondimensionalized wave amplitude, A, solid; B^S, dash; B^A, dot-dash. (b) Flux densities, $A - B^S$, dot-dash; $A - B^A$, dash; $B^S - B^A$, dot; nonlinear term, solid. (c) The total velocity at the top of the troposphere and (d) The total velocity at the bottom of the troposphere for the example shear from Figure 5 and Section 5.1 at the initial time.

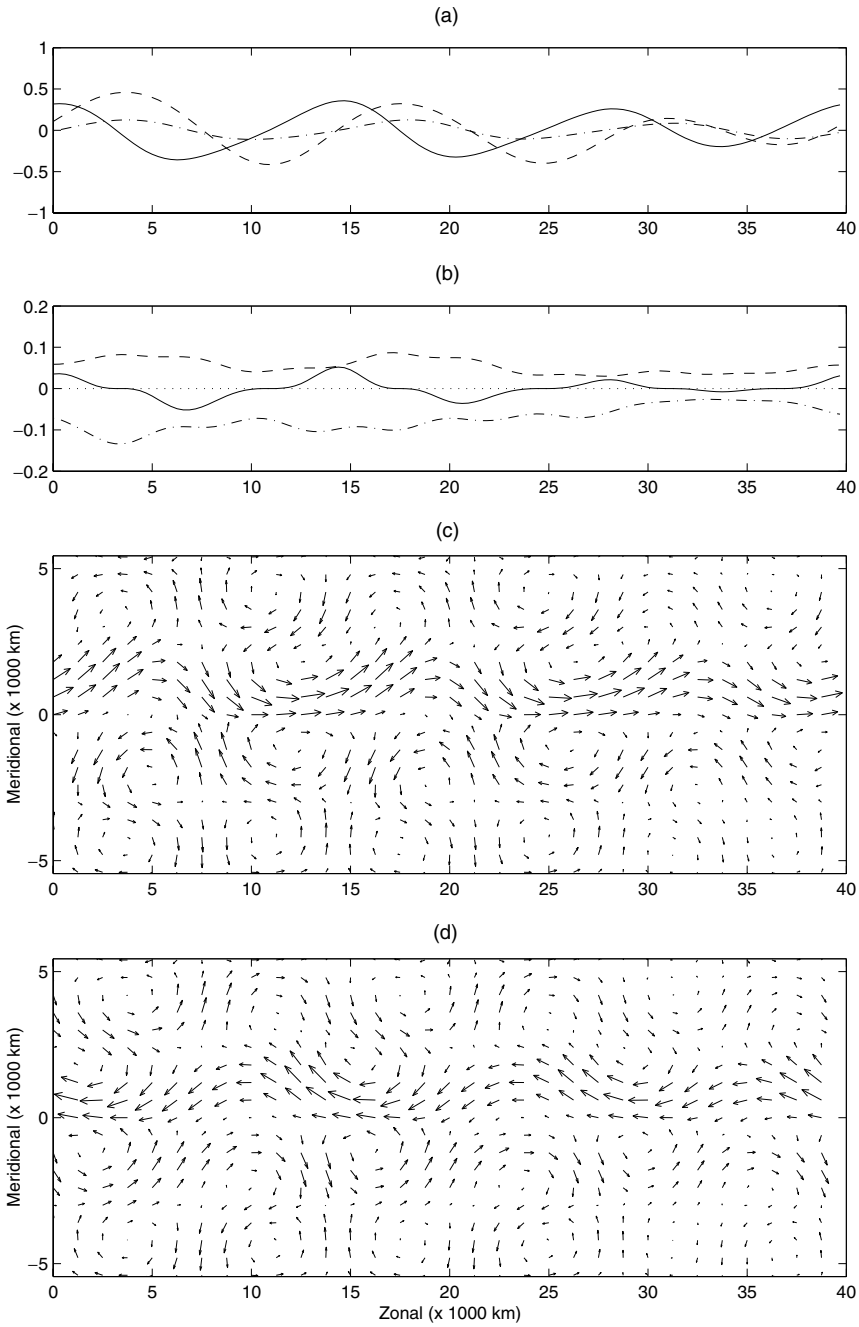

Figure 7. (a) Nondimensionalized wave amplitude, A, solid; B^S, dash; B^A, dot-dash. (b) Flux densities, $A - B^S$, dot-dash; $A - B^A$, dash; $B^S - B^A$, dot; nonlinear term, solid. (c) The total velocity at the top of the troposphere and (d) The total velocity at the bottom of the troposphere for the example shear from Figure 5 and Section 5.1 at 10 days.

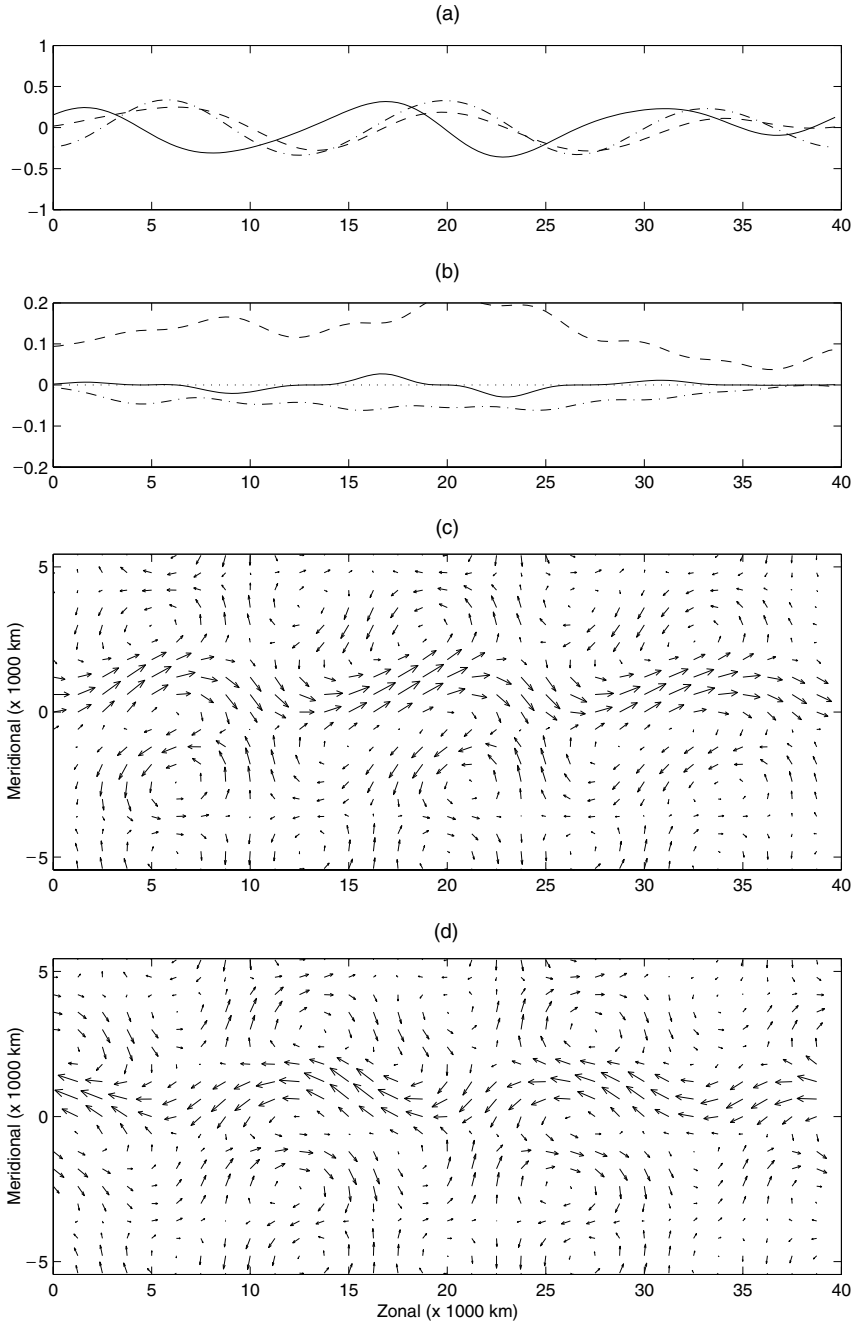

Figure 8. (a) Nondimensionalized wave amplitude, A, solid; B^S, dash; B^A, dot-dash. (b) Flux densities, $A - B^S$, dot-dash; $A - B^A$, dash; $B^S - B^A$, dot; nonlinear term, solid. (c) The total velocity at the top of the troposphere and (d) The total velocity at the bottom of the troposphere for the example shear from Figure 5 and Section 5.1 at 20 days.

We conclude that if there is sufficiently strong asymmetry in the baroclinic shear then antisymmetric barotropic waves are driven strongly enough to inhibit the development of symmetric equatorial baroclinic waves. Furthermore we have discussed how the nonlinear drive of baroclinic waves is proportional to the zonal barotropic velocity at the equator. The barotropic waves are essentially shifted northward in this example and organize to have a very weak zonal velocity at the equator. This quenches any nonlinear driving of the baroclinic waves and the winds are dominated by barotropic waves for long times.

5.2. Equatorial baroclinic waves driving antisymmetric barotropic waves

In this example we study the effect of antisymmetric baroclinic and barotropic shears on the exchange of energy from baroclinic waves to barotropic waves. The zonal velocity profile is a sum of three components and is shown in Figure (9) at the top and bottom of the troposphere. Two have the meridional structure of an $m = 1$ and $m = 2$ baroclinic wave each with a 5 ms^{-1} maximum zonal velocity. The third is an antisymmetric barotropic wind whose zonal velocity is proportional to $\sin(\sqrt{5}y)$ with a maximum of 2.5 ms^{-1}. The maximum of the zonal wind at the bottom and minimum at the top of the troposphere occur around 1000 km north. The initial condition, shown in Figure (10), is a purely baroclinic wave and a jet is evident at about 1000 km north in Figure 10(c). From Figure 9(c), note that baroclinic energy is rapidly converted to barotropic waves, primarily antisymmetric. After long times approximately equal amounts of energy reside in the baroclinic and antisymmetric barotropic modes.

For physical applications we are primarily interested in early times. At 10 days, Figure 11(a), the baroclinic wave has been greatly depleted over much of the domain in favor of the antisymmetric barotropic wave. The energy flux in Figure 11(b) indicates that the baroclinic waves are being depleted most strongly at their extrema. Barotropic cyclones centered at 1000 km north dominate the winds around $x = 15$. There is no longer any significant energy exchange at 16 days, as is evidenced in Figure 12(b). The amplitude of the symmetric barotropic wave is approximately -0.6 times the antisymmetric barotropic wave over most of the domain and using Equation (21) we find that it corresponds to a shift of the centerline of the barotropic waves to about 900 km north. We can conclude that the maximum of the baroclinic shear serves to set an origin for the barotropic waves but does not inhibit the transport of energy from baroclinic waves to barotropic waves. The barotropic waves tend to align themselves symmetrically about the maximum of a baroclinic zonal shear.

5.3. Purely antisymmetric shear driving asymmetric waves

As an instructive theoretical example we consider a purely antisymmetric baroclinic shear and antisymmetric barotropic wind with an initially antisymmetric

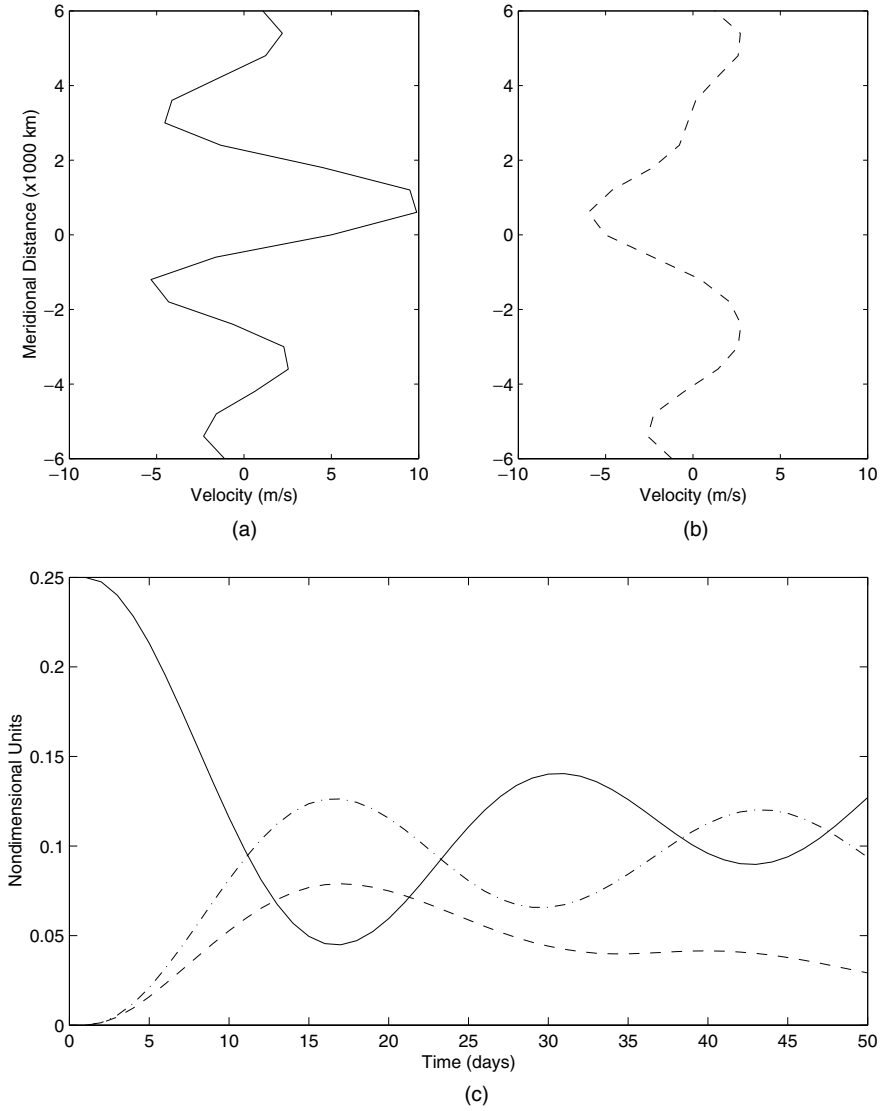

Figure 9. Zonal mean velocity (a) bottom and (b) top of troposphere for the example in Section 5.2 with a 5 $\mathrm{m\,s^{-1}}$ antisymmetric baroclinic shear, a 5 $\mathrm{m\,s^{-1}}$ symmetric shear and a 2.5 $\mathrm{m\,s^{-1}}$ antisymmetric barotropic wind. (c) The energy in the symmetric barotropic (B^S, dash), symmetric baroclinic (A, solid) and antisymmetric barotropic waves (B^A, dot-dash) as a function of time.

barotropic wave profile. Figure 13 shows that there are large variations in the winds at the bottom of the troposphere and more moderate variations at the top. Within 20 days Figure 13(c) shows that most of the energy exchange has occurred and the system becomes quasi-stationary.

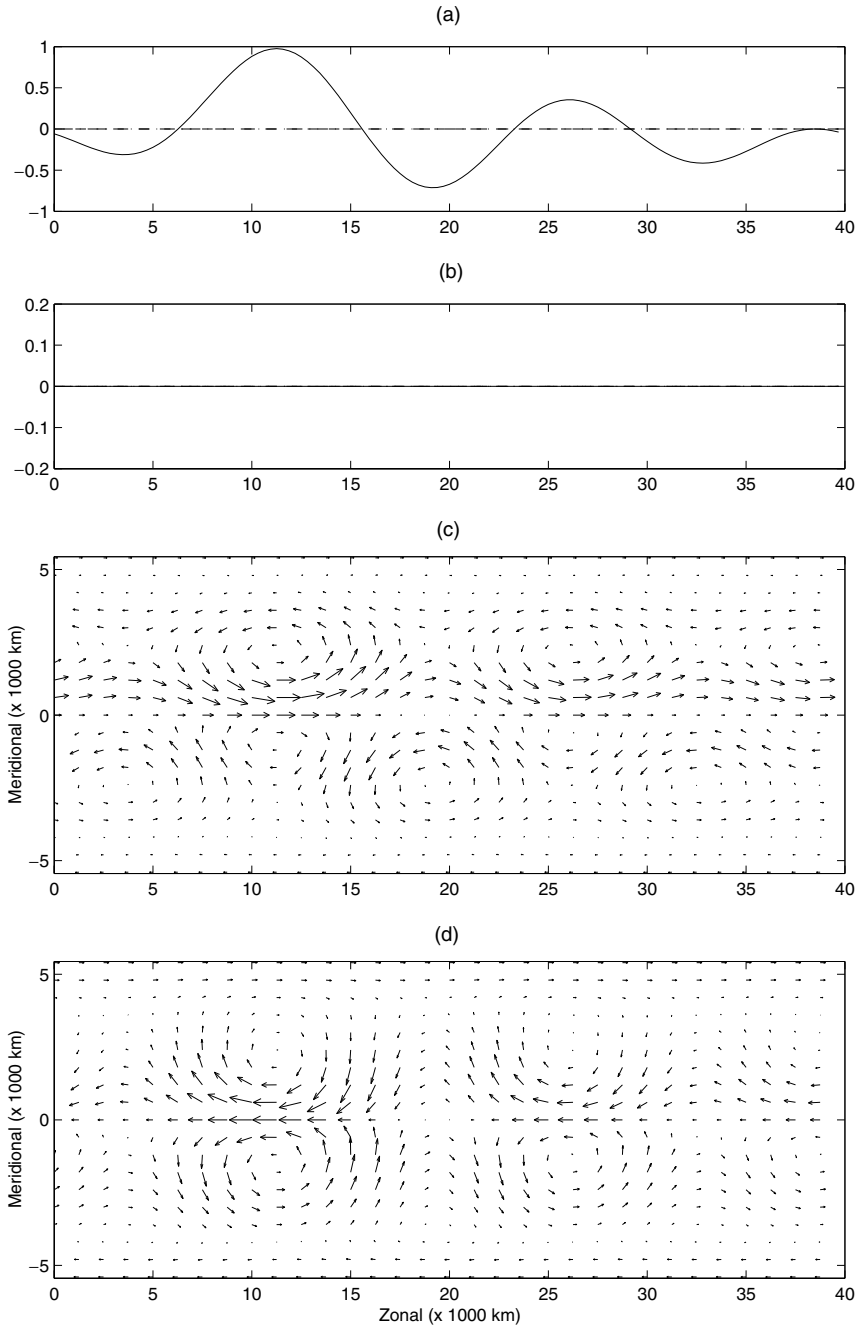

Figure 10. (a) Nondimensionalized wave amplitude, A, solid; B^S, dash; B^A, dot-dash. (b) Flux densities, $A - B^S$, dot-dash; $A - B^A$, dash; $B^S - B^A$, dot; nonlinear term, solid. (c) The total velocity at the top of the troposphere and (d) The total velocity at the bottom of the troposphere for the example shear from Figure 9 and Section 5.2 at the initial time.

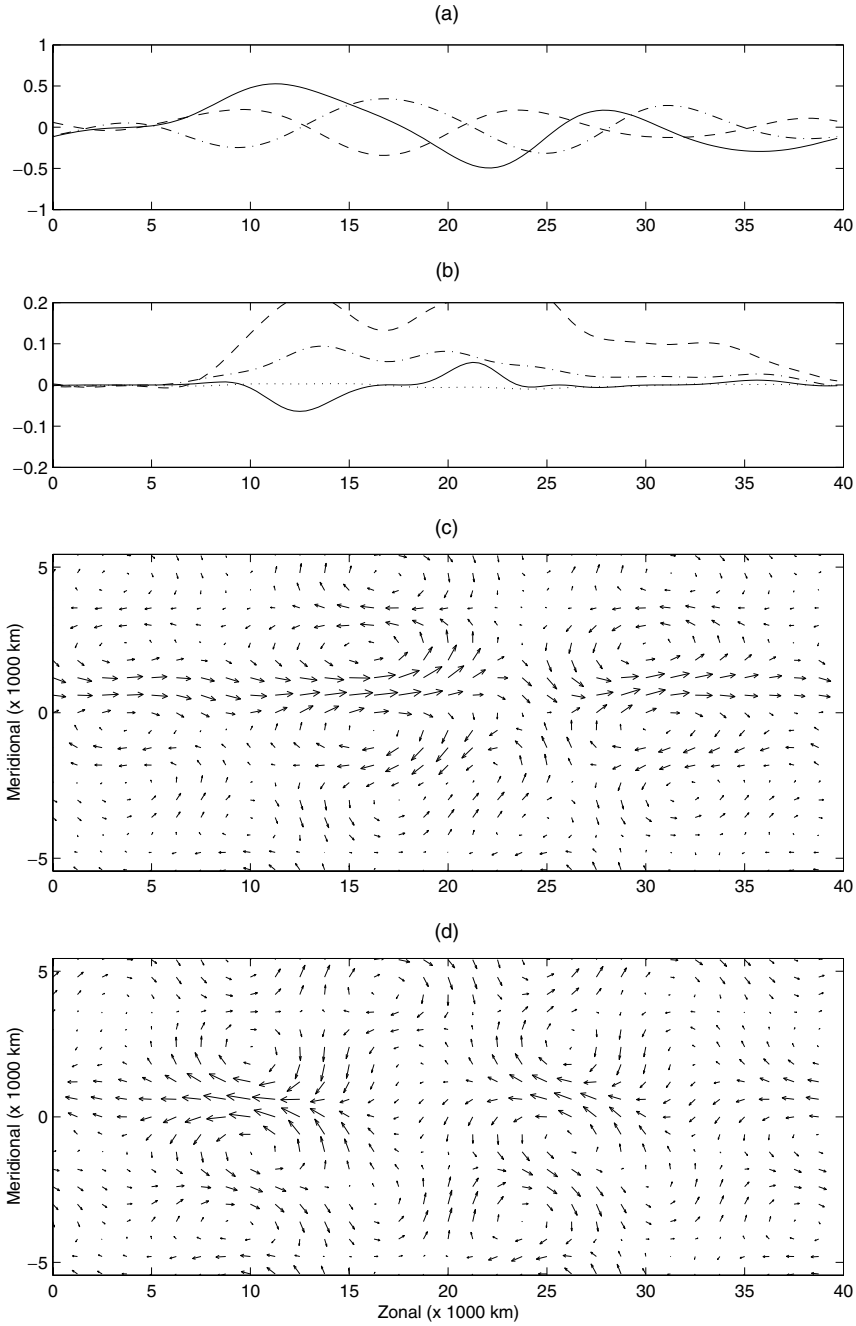

Figure 11. (a) Nondimensionalized wave amplitude, A, solid; B^S, dash; B^A, dot-dash. (b) Flux densities, $A - B^S$, dot-dash; $A - B^A$, dash; $B^S - B^A$, dot; nonlinear term, solid. (c) The total velocity at the top of the troposphere and (d) The total velocity at the bottom of the troposphere for the example shear from Figure 9 and Section 5.2 at 10 days.

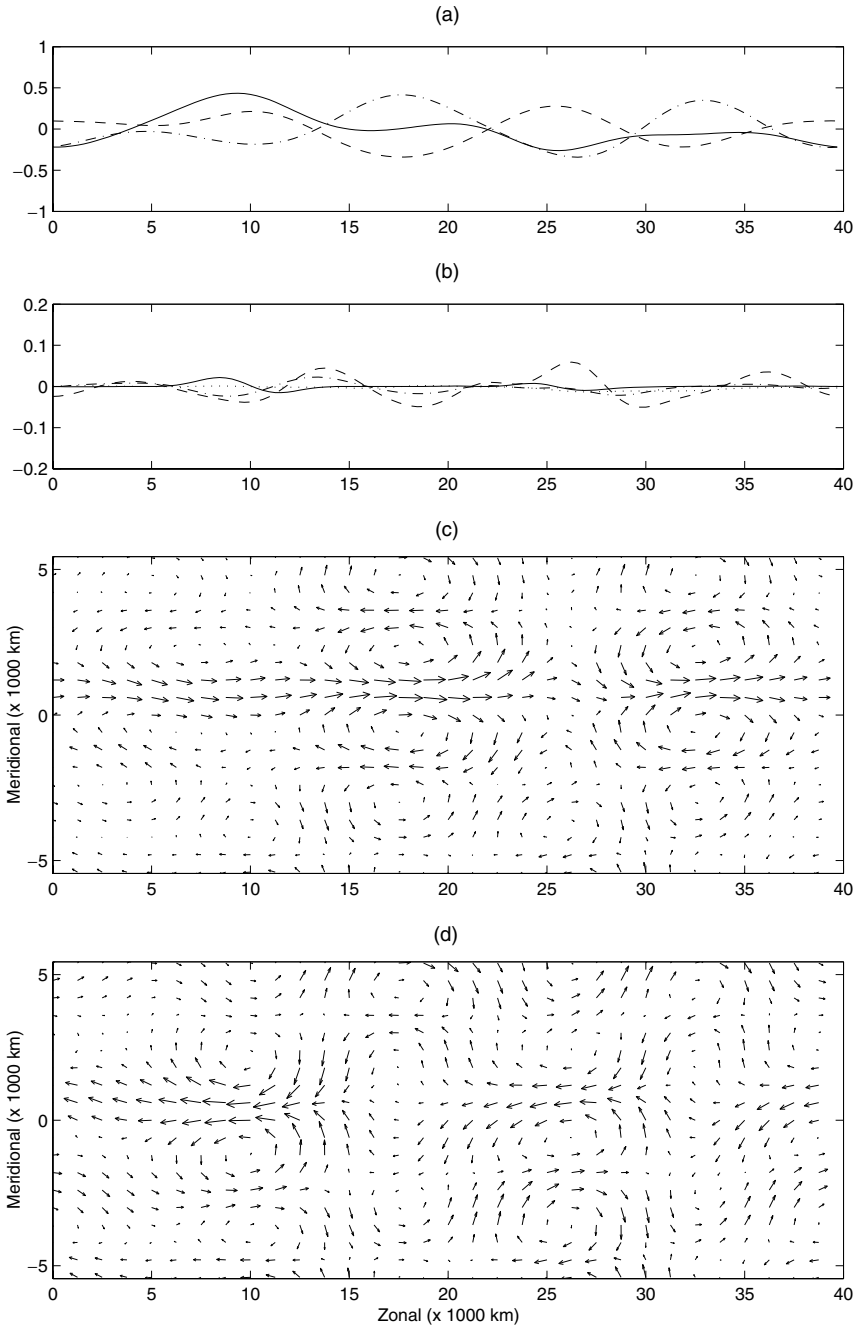

Figure 12. (a) Nondimensionalized wave amplitude, A, solid; B^S, dash; B^A, dot-dash. (b) Flux densities, $A - B^S$, dot-dash; $A - B^A$, dash; $B^S - B^A$, dot; nonlinear term, solid. (c) The total velocity at the top of the troposphere and (d) The total velocity at the bottom of the troposphere for the example shear from Figure 9 and Section 5.2 at 16 days.

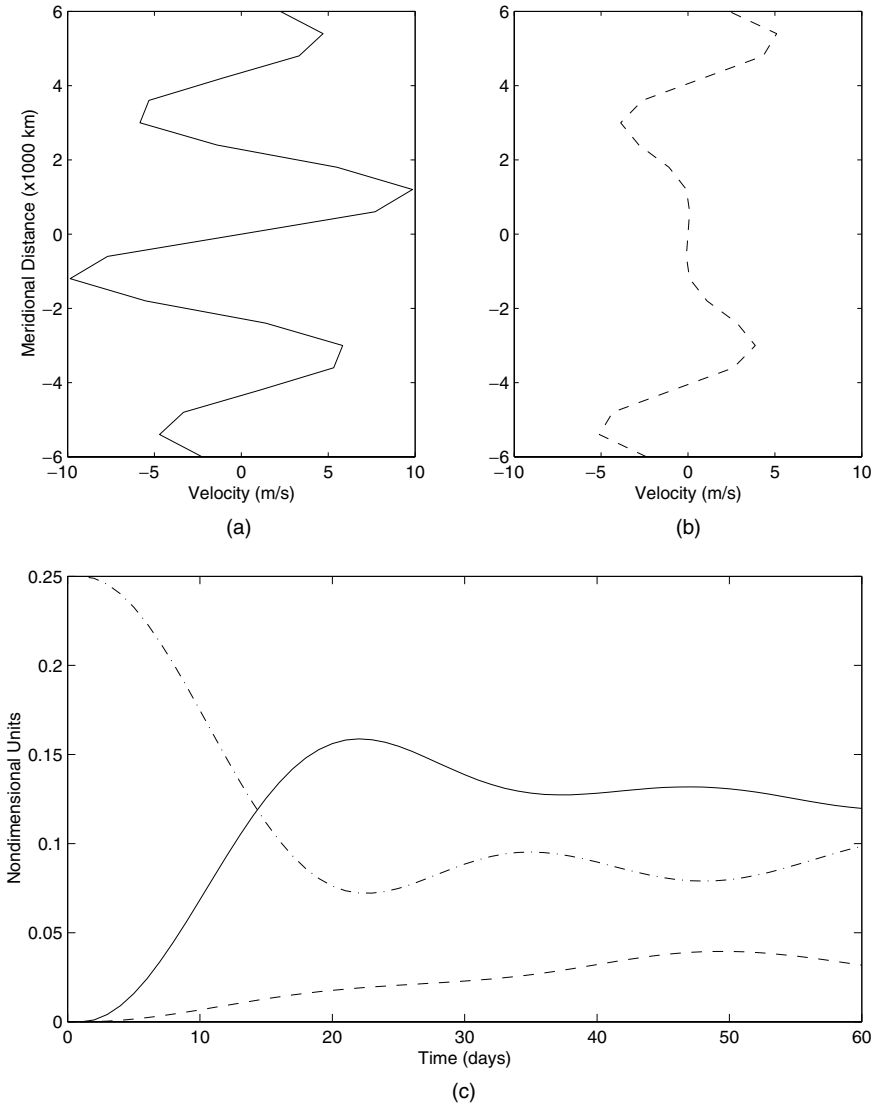

Figure 13. Zonal mean velocity (a) bottom and (b) top of troposphere for the purely antisymmetric mean flow from Section 5.3 with 5 $\mathrm{m\,s^{-1}}$ antisymmetric baroclinic shear and a 5 $\mathrm{m\,s^{-1}}$ antisymmetric barotropic wind. (c) The energy in the symmetric barotropic (B^S, dash), symmetric baroclinic (A, solid) and antisymmetric barotropic waves (B^A, dot-dash) as a function of time.

In Figure 14 the initial velocity has an antisymmetric barotropic wave pair localized near $x = 10$. By 10 days there is a very strong pumping of baroclinic waves coming from the leading vortex in Figure 15(b). The velocity at the bottom (Figure 15(c)) is dominated by the two oppositely oriented jets of the

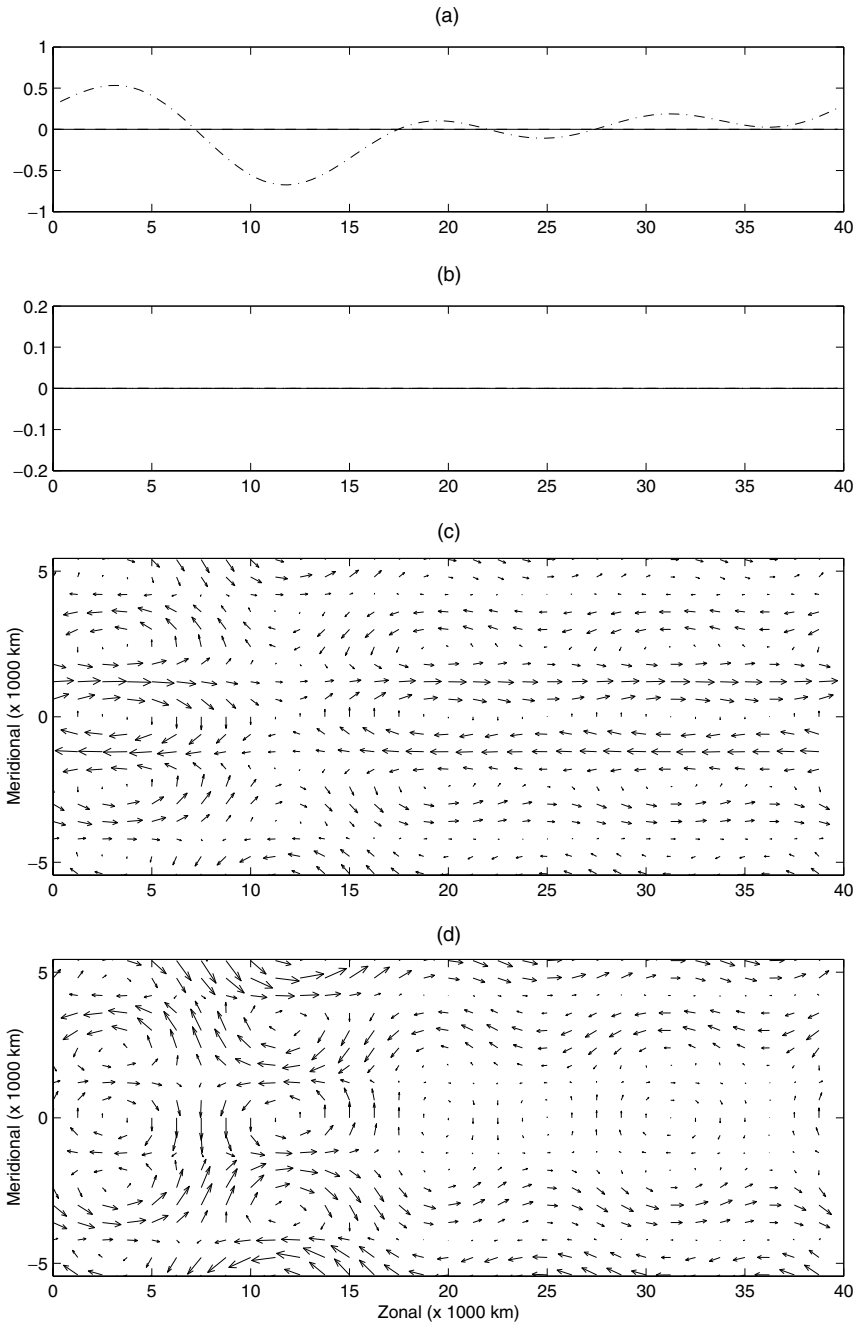

Figure 14. (a) Nondimensionalized wave amplitude, A, solid; B^S, dash; B^A, dot-dash. (b) Flux densities, $A - B^S$, dot-dash; $A - B^A$, dash; $B^S - B^A$, dot; nonlinear term, solid. (c) The total velocity at the top of the troposphere and (d) The total velocity at the bottom of the troposphere for the example shear from Figure 13 and Section 5.3 at the initial time.

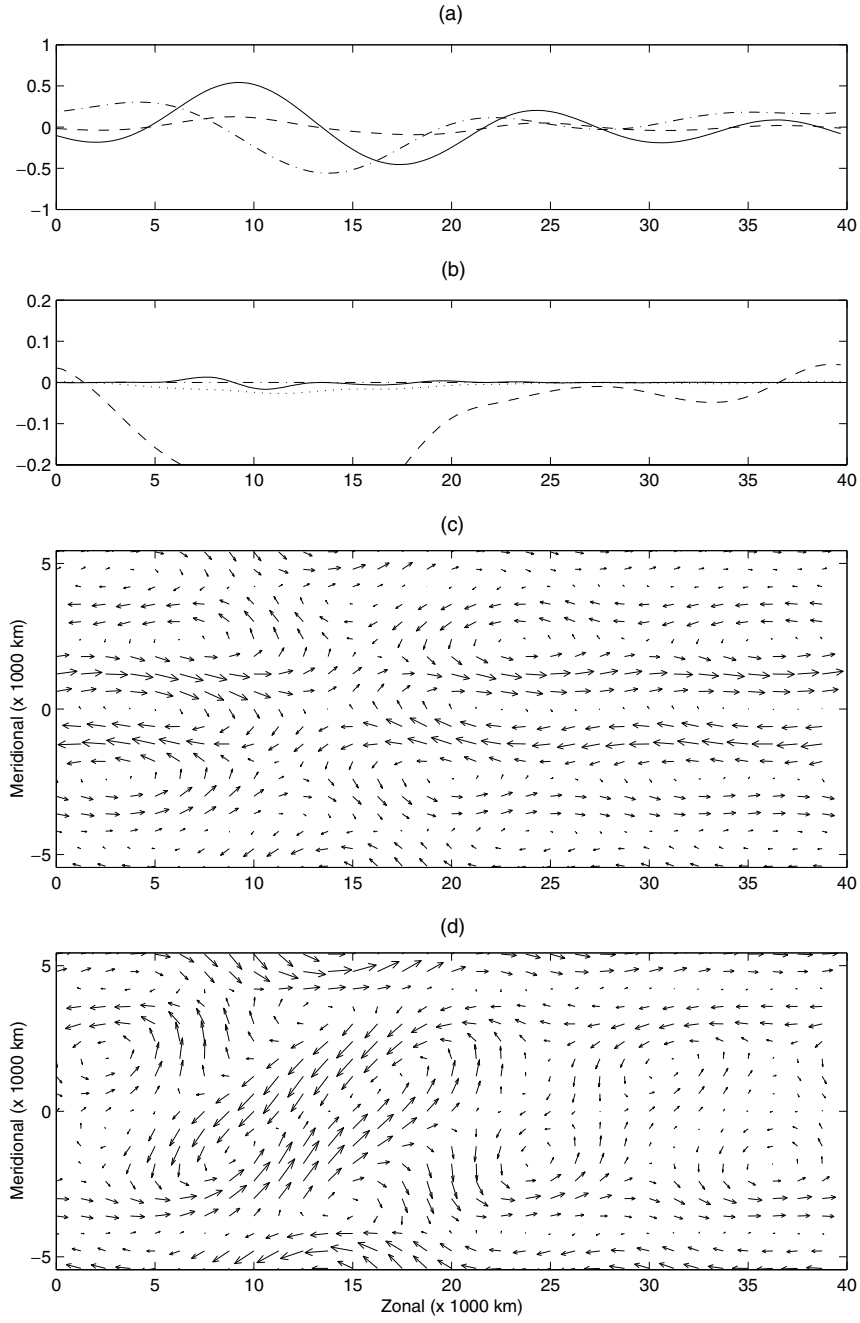

Figure 15. (a) Nondimensionalized wave amplitude, A, solid; B^S, dash; B^A, dot-dash. (b) Flux densities, $A - B^S$, dot-dash; $A - B^A$, dash; $B^S - B^A$, dot; nonlinear term, solid. (c) The total velocity at the top of the troposphere and (d) The total velocity at the bottom of the troposphere for the example shear from Figure 13 and Section 5.3 at 10 days.

mean shear. However there is a dramatically tilted vortex at the top of the troposphere in Figure 15(d). This is a strong north–south connection across the equator and there is also a strong wind at midlatitudes near the vortex, an indication of the persistence of the barotropic wave. Figure 16(d) shows that at 18 days this vortex has broken up in the upper troposphere into a cyclonic vortex in the northern hemisphere and an anticyclonic one in the southern hemisphere. Both vortices have no partner in the opposite hemisphere, which is an indication of the asymmetry of the winds. At the top of the troposphere these vortices are sitting at latitudes where there is a very weak zonal mean velocity. At the bottom of the troposphere, these waves do not produce vortices, but rather weaken the jet over which they sit.

In summary baroclinic shear has the effect of setting a latitude about which the barotropic waves become symmetric; that of the maximum of the baroclinic shear. If the antisymmetric component is too strong there is a tendency to draw energy away from the baroclinic waves. The addition of an antisymmetric barotropic shear also forces the latitude of symmetry northward but does not seem to affect barotropic–baroclinic energy exchange. A zonal shear that is entirely antisymmetric yields a quasistationary and highly asymmetric velocity field consisting of $m = 1$ baroclinic waves and antisymmetric barotropic waves.

6. Solitary waves in mean shears

When the baroclinic shear has the same meridional structure as the baroclinic waves and the barotropic zonal wind is meridionally symmetric and has the same wavenumber as the barotropic waves we can use the convention of Ref. [1] and not require the zonal means of the waves to vanish. The zonal means then describe the mean baroclinic shear and barotropic wind and the BSAB equations reduce to the equations derived in Ref. [1]

$$\begin{aligned} A_\tau - DA_{xxx} + (AB^S)_x &= 0 \\ B^S_\tau - B^S_{xxx} + AA_x &= 0 \end{aligned} \tag{50}$$

plus a linear dispersion equation for B^A, which has been omitted because we shall assume zero initial data for this wave. Our interest is in the $m = 1$ symmetric baroclinic wave interacting with the symmetric $l = \sqrt{3}$ barotropic wave for which $D = 0.889$ and the $m = 2$ antisymmetric baroclinic wave interacting with the symmetric $l = \sqrt{5}$ barotropic wave for which $D = 0.96$. The equations in (50) do not have nonlinear self-interaction as in Korteweg–de Vries (KdV) but the two modes exchange energy through the quadratic nonlinearity; thus we still can seek localized solutions in the form of $\mathrm{sech}^2(\xi)$ for each component, as for KdV solitary waves. For the purposes of this discussion we will let the x-domain be infinite and restrict ourselves to solutions, which are localized

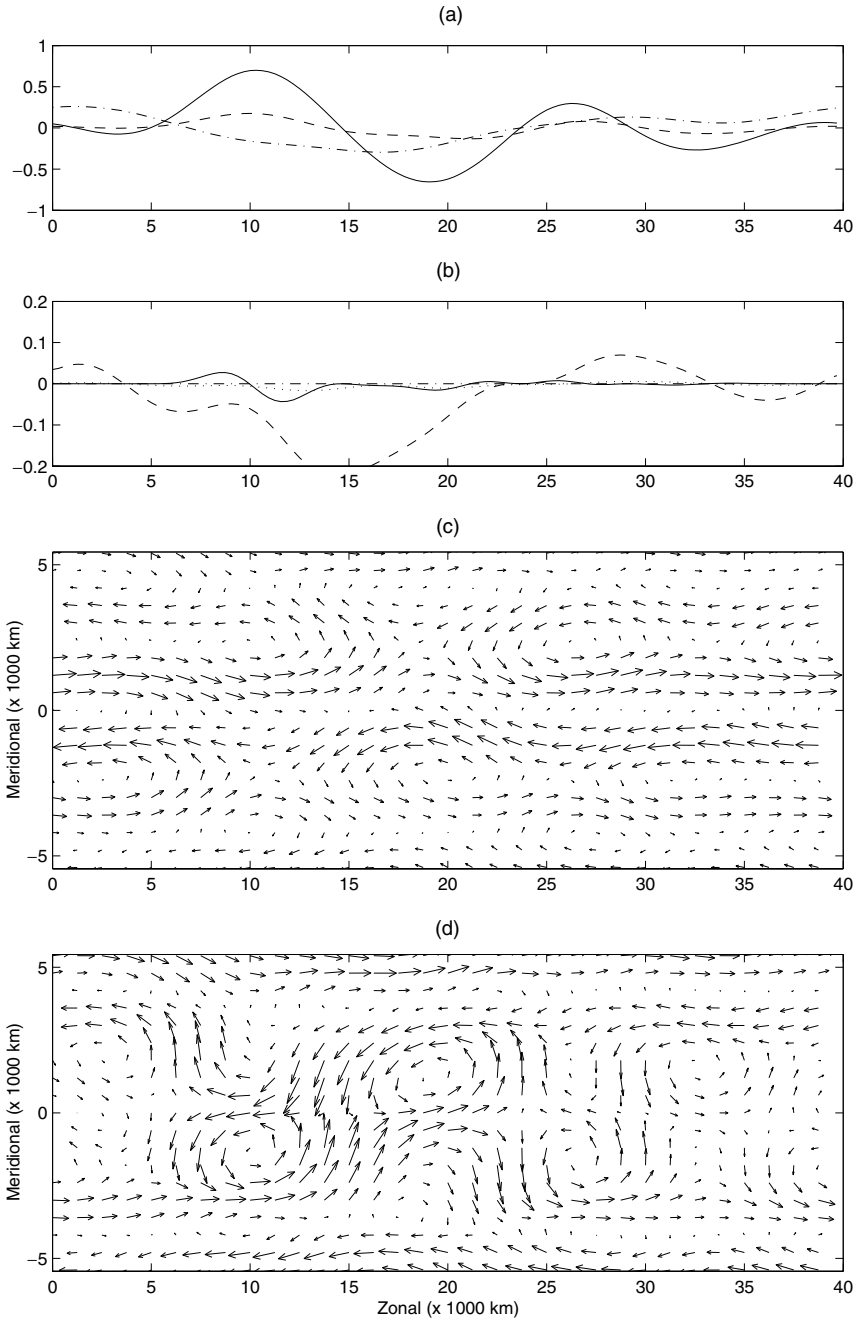

Figure 16. (a) Nondimensionalized wave amplitude, A, solid; B^S, dash; B^A, dot-dash. (b) Flux densities, $A - B^S$, dot-dash; $A - B^A$, dash; $B^S - B^A$, dot; nonlinear term, solid. (c) The total velocity at the top of the troposphere and (d) The total velocity at the bottom of the troposphere for the example shear from Figure 13 and Section 5.3 at 18 days.

enough not to be affected by the actual periodicity of the Earth. We seek traveling waves of the form

$$\begin{aligned} A(x-ct) &= a\,\mathrm{sech}^2\left(\frac{x-ct}{\lambda}\right)+\bar{A} \\ B^S(x-ct) &= -b\,\mathrm{sech}^2\left(\frac{x-ct}{\lambda}\right)+\bar{B}. \end{aligned} \tag{51}$$

and upon substituting into (50) we find that such solutions exist if

$$\begin{aligned} b &= \frac{6D}{\lambda^2} \\ \bar{B}a-\bar{A}b &= a\left(c+\frac{4D}{\lambda^2}\right) \\ \frac{a^2}{2} &= \frac{6b}{\lambda^2} \\ -a\bar{A} &= \left(c+\frac{4}{\lambda^2}\right)b. \end{aligned} \tag{52}$$

These equations should be thought of as a relationship between the solitary wave amplitudes, size, and speed, a, b, λ, c, respectively, and the zonal baroclinic shear $\bar{A}$, barotropic wind, $\bar{B}$ and ratio of dispersions, D. The first equation in (52) implies $b > 0$ and upon substitution into the third,

$$a = \pm b\sqrt{\frac{2}{D}} \equiv \pm rb \tag{53}$$

where $r = 3/2$ when $m = 1$ and $r = 5/(2\sqrt{3})$ when $m = 2$. Therefore, there are two families of solitary waves, one for each sign of a. Upon substitution into the remaining two equations we can eliminate a and b arriving at two linear, inhomogeneous equations in c and λ^{-2}. Their solution for arbitrary m are the wavelength and speed of the positive and negative baroclinic waves,

$$\begin{aligned} \lambda^2 &= \frac{4r(1-D)}{\mp(r^2-1)\bar{A}-r\bar{B}} \\ c &= \frac{\pm\bar{A}+r\bar{B}}{r(1-D)} \end{aligned} \tag{54}$$

and specifically,

$$\begin{array}{cc} m=1 & m=2 \\ \lambda^2 = \frac{8}{3(\mp 5\bar{A}-6\bar{B})} & \lambda^2 = \frac{8\sqrt{3}}{5(\mp 13\bar{A}-10\sqrt{3}\bar{B})} \\ c = \pm 6\bar{A}+9\bar{B} & c = \pm 10\sqrt{3}\bar{A}+25\bar{B} \end{array} \tag{55}$$

where the top signs in (54) and (55) are for $a > 0$ and the bottom signs for $a < 0$. In these solutions a is given by (53) and b by the first relation in (52). Thus the parameter plane $\bar{A} - \bar{B}$ is divided up as follows

$$\begin{array}{ccc} m = 1 & & m = 2 \\ \bar{B} > \frac{5}{6}|\bar{A}| & \text{no solutions} & \bar{B} > \frac{13}{10\sqrt{3}}|\bar{A}| \\ -\frac{5}{6}|\bar{A}| < \bar{B} < \frac{5}{6}|\bar{A}| & \text{1 solution} & -\frac{13}{10\sqrt{3}}|\bar{A}| < \bar{B} < \frac{13}{10\sqrt{3}}|\bar{A}| \\ \bar{B} < -\frac{5}{6}|\bar{A}| & \text{2 solutions} & \bar{B} < -\frac{13}{10\sqrt{3}}|\bar{A}|. \end{array} \tag{56}$$

These can be expressed in dimensional units using the relations in Appendix B, the values of δ, ϵ, and the dimensional units in (5), but we shall dispense with this for such general cases because the expressions are cumbersome and uninformative. Instead we construct two solitary waves for each m and discuss their resilience against collisions. In these examples we will explicitly indicate the physical and nondimensional parameters.

6.1. Solitary waves: Examples and collisions

For any zonal mean baroclinic shear, $\bar{A}$, and mean barotropic shear, $\bar{B}$, there exist at most two solitary waves of the form of Equation (51), one with positive baroclinic amplitude the other with negative. When $m = 1$ the rescaling parameters, dry gravity wave speed ($c = 50\ \mathrm{m\,s^{-1}}$) and choice of $\epsilon = 0.1$ yield the following relationships between nondimensional and dimensional values. A domain length of 14 in Equation (50) corresponds to 40,000 km, the circumference of the earth, and one nondimensional time unit is 22 days. Therefore wavelength $\lambda = 1$ corresponds to a length of 2850 km, equivalently 5700 km width from the points at one e-folding from the maximum, and a nondimensional solitary wave speed of 1 is equal to $1.5\ \mathrm{m\,s^{-1}}$. For the amplitude rescalings a velocity of $5\ \mathrm{m\,s^{-1}}$ is attained at the equator by a baroclinic amplitude of $A = 1.1$ or a barotropic amplitude of $B^S = 1.35$.

Figures 17 and 18 show the two $m = 1$ solitary waves which occur when the mean barotropic shear velocity is $-1\ \mathrm{m\,s^{-1}}$ and the mean baroclinic shear velocity is $-0.9\ \mathrm{m\,s^{-1}}$.

When $a < 0$ both the baroclinic and barotropic amplitudes are negative, corresponding to westward winds at the bottom of the troposphere near the equator. The wave in Figure 17 is 11,400 km long and travels at $-18.7\ \mathrm{m\,s^{-1}}$ with respect to the ground. The maximum wind speeds are $-9.1\ \mathrm{m\,s^{-1}}$ for the baroclinic component and $-5.0\ \mathrm{m\,s^{-1}}$ for the barotropic component giving -14.1 and $4.1\ \mathrm{m\,s^{-1}}$ at the bottom and top of the troposphere, respectively. In this instance, the velocity field consists of a strong anticyclone pair near the equator at the bottom of the troposphere and a weaker cyclone pair at midlatitudes at the top of the troposphere.

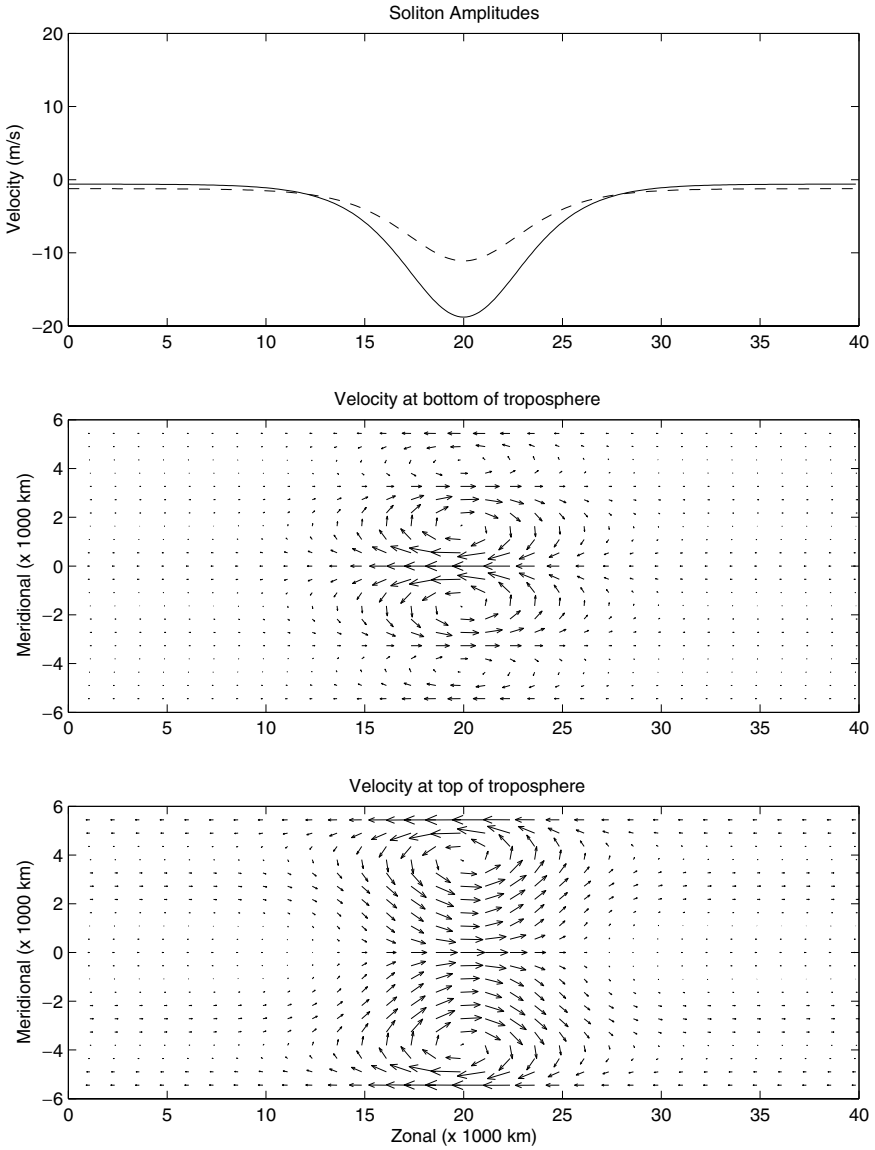

Figure 17. The amplitude (including mean flows) and velocity field (top and bottom) of an $m = 1$, 11,400 km solitary wave traveling at -18.7 ms^{-1} wave whose baroclinic and barotropic components are both westward at the bottom of the troposphere at the equator. The barotropic amplitude is dashed and the baroclinic amplitude is a solid curve.

When $a > 0$ the baroclinic and barotropic wind velocities oppose one another at the bottom of the troposphere. The corresponding wave in Figure 18 is 5,700 km in extent and travels at -22.3 ms^{-1} (westward) with respect to the stationary frame. The maximum wind speeds are 36 ms^{-1} for the baroclinic

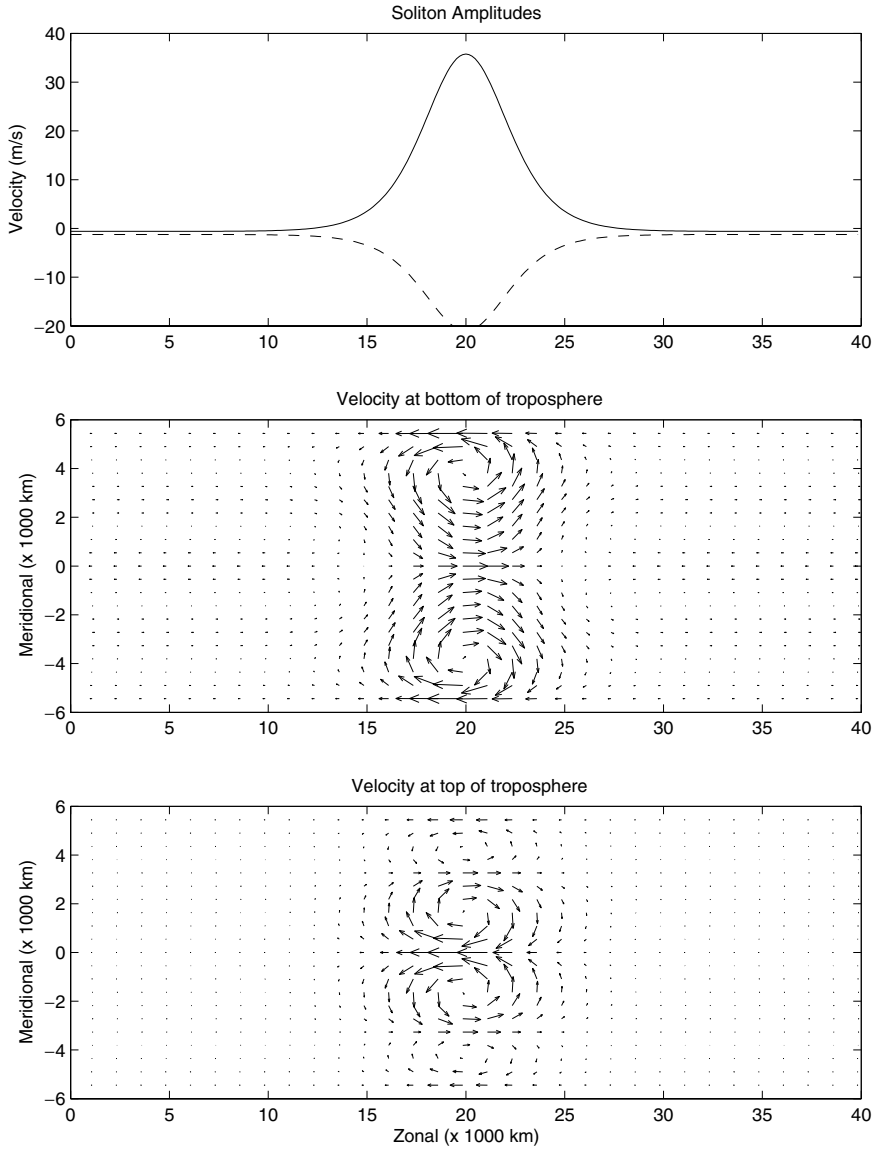

Figure 18. The amplitude (including mean flows) and velocity field (top and bottom) of an $m = 1{,}5700$ km solitary traveling at -22.3 ms^{-1} wave whose baroclinic and barotropic components are in opposite directions bottom of the troposphere at the equator. The barotropic amplitude is dashed and the baroclinic amplitude is a solid curve.

component and -20 ms^{-1} for the barotropic component meaning that the maximum speeds are 16 and -56 ms^{-1} at the bottom and top of the troposphere, respectively. The velocity field consists of a cyclone pair at midlatitudes at the bottom and an anticyclone pair concentrated near the equator at the top of

the troposphere. Though the wind velocities are unphysically large, it is the only other soliton that exists with the same mean shears as the first soliton (Figure 17) and is used next to study their stability under collisions.

To test the stability of solitary waves to collisions a domain of twice the circumference of the earth is initialized with these two waves separated by 40,000 km. This length is chosen to ensure that the tails of the waves are well separated and the BSAB equations are integrated using 512 modes. As a diagnostic we use the root mean square relative difference in the amplitudes,

$$\text{Error} = \sqrt{\frac{(A(x',t) - A(x,0))^2 + (B^S(x',t) - B^S(x,0))^2}{A(x,0)^2 + B^S(x,0)^2}} \tag{57}$$

where x' is chosen to overlay each of the individual waves. After two collisions each wave remains largely intact, the error being less than 2.5%. Furthermore, each collision imparts a 6700 km eastward phase shift to the longer wave while apparently no phase shift occurs in the shorter wave.

When $m = 2$ the parameters in Appendix B give, for Equation (50), a domain length of 15.25 for the 40,000 km circumference of the Earth, one nondimensional time unit for 46 days and 0.65 $\mathrm{m\,s^{-1}}$ for a nondimensional wave velocity of one. The baroclinic wave, and therefore, baroclinic mean shear have zero zonal velocity at the equator when $m = 2$, thus the first maximum is chosen as a measure of the wave strength. Therefore a baroclinic amplitude of 1.3 corresponds to a zonal velocity of 5 $\mathrm{ms^{-1}}$ at the first maximum of the $m = 2$ eigenfunction, Equation (13). A barotropic amplitude of -1.2 corresponds to a 5 $\mathrm{ms^{-1}}$ zonal velocity, because $\mathrm{sgn}(\alpha) < 0$.

Figures 19 and 20 show $m = 2$ solitary waves in the presence of very weak mean shears. The mean barotropic wind is -0.25 $\mathrm{ms^{-1}}$ and the mean baroclinic wind is 0.1 $\mathrm{ms^{-1}}$ at their maxima. For $m = 2$ the equatorial Rossby wave speed is $c_2 = -10$ $\mathrm{ms^{-1}}$ and the wave amplitudes are referred to this moving frame. The solitary wave in Figure 19 has a barotropic amplitude of 6.1 $\mathrm{ms^{-1}}$, a baroclinic amplitude of 7.8 $\mathrm{ms^{-1}}$, and travels at -10.7 $\mathrm{ms^{-1}}$ with respect to the ground. The wave in Figure 20 has a barotropic amplitude of 12 $\mathrm{ms^{-1}}$, a baroclinic amplitude of -15.8 $\mathrm{ms^{-1}}$ and travels at $-11/3$ $\mathrm{ms^{-1}}$ with respect to the ground. Both flows are invariant under simultaneous exchange of top/bottom and north/south. Focusing on Figure 19 at the bottom of the troposphere there is an eastward jet just north of the equator and a westward jet at around 2000 km south. There is a clear vortex between the two jets and another vortex south of the second one. The top of the troposphere has the same pattern, but with north and south reversed. It is striking that the zonal velocity is weakest at the top of the troposphere above the latitudes where it is strongest at the bottom of the troposphere. The solitary wave in Figure 20 has all of the same features with top and bottom reversed.

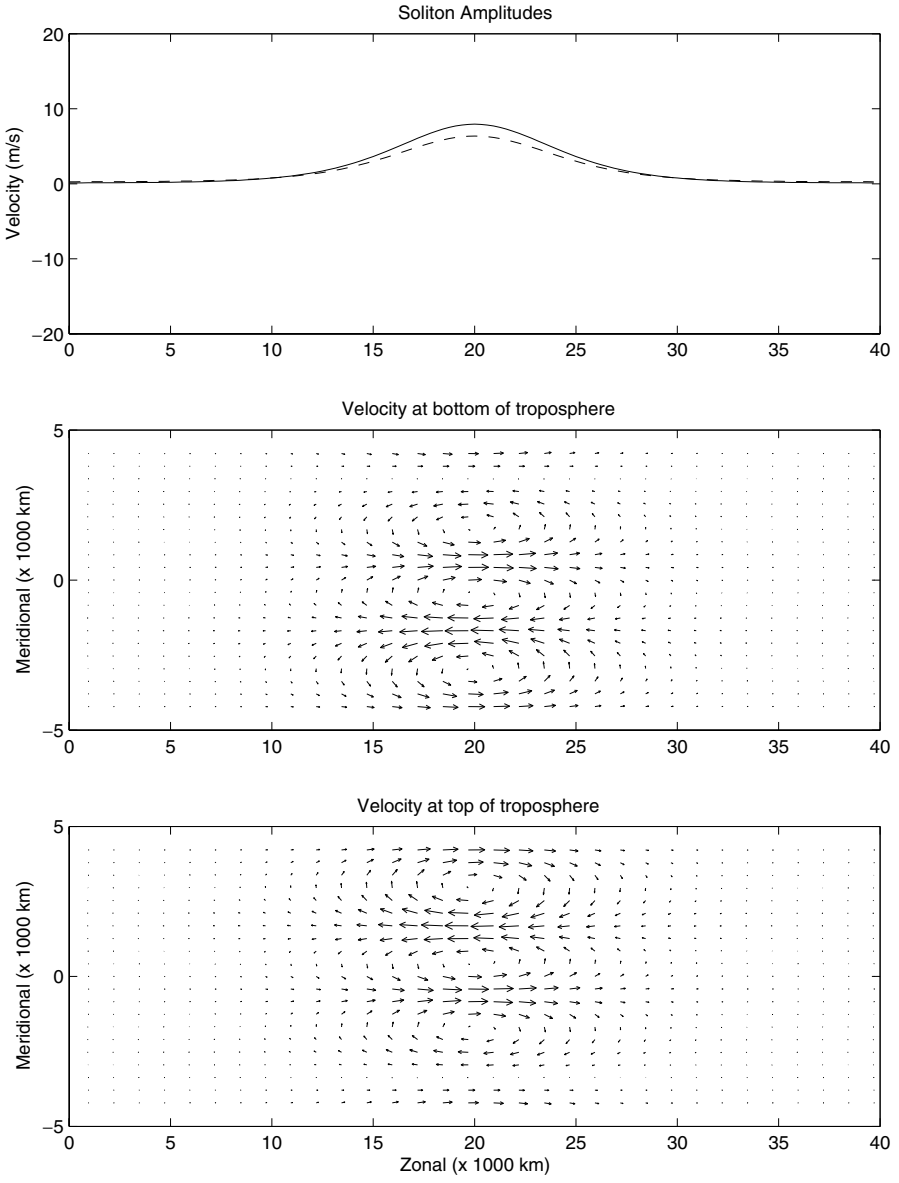

Figure 19. The amplitude (including mean flows) and velocity field (top and bottom) of an $m = 2$, 10,500 km solitary wave traveling at $-10.7\ \mathrm{m\,s^{-1}}$ with a maximum wind velocity of $12\ \mathrm{m\,s^{-1}}$. The barotropic amplitude is dashed and the baroclinic amplitude is a solid curve.

We have presented two solitary waves in parameter regimes relevant to atmospheric science for each of a symmetric, $m = 1$ baroclinic wave interacting with an $l = \sqrt{3}$ symmetric barotropic wave and an antisymmetric, $m = 2$, baroclinic waves interacting with an $l = \sqrt{5}$ symmetric barotropic wave.

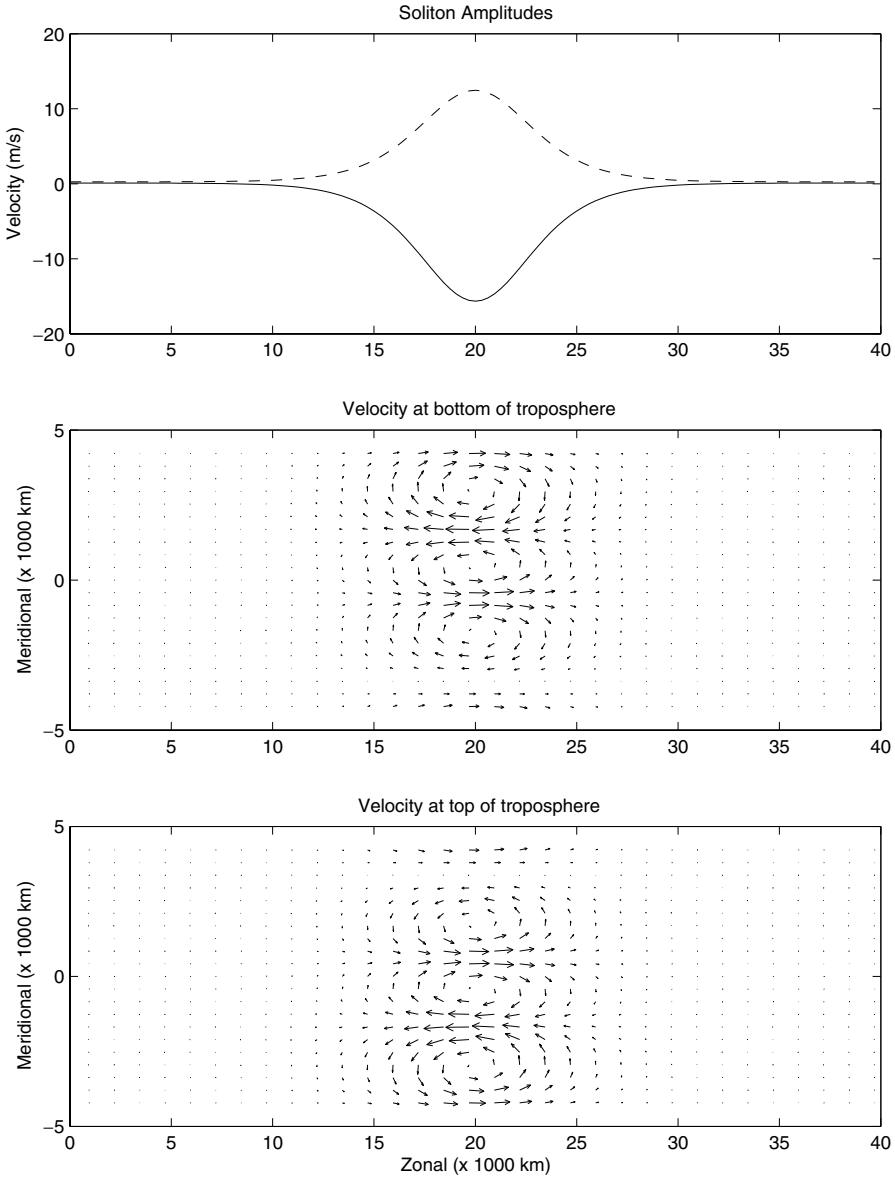

Figure 20. The amplitude (including mean flows) and velocity field (top and bottom) of an $m = 2$, 7400 km solitary wave traveling at -11.3 ms^{-1} with a maximum wind velocity of 22 ms^{-1}. The barotropic amplitude is dashed and the baroclinic amplitude is a solid curve.

Numerical results suggest that these waves may be stable to collisions with one another, but are not conclusive on this point. Furthermore, we have only examined a particular set of analytic traveling wave solutions and found that up to two can exist for any prescribed mean barotropic and baroclinic shear.

Whether or not nonanalytic traveling waves exist for the same values of the mean wind and shear is also an open question. Both of these latter points are beyond the scope of this paper but merit further investigation.

7. Concluding discussion

We have derived equations governing the resonant interaction of nearly dispersionless equatorially confined baroclinic Rossby waves and barotropic Rossby waves with a significant midlatitude projection. The result is three linearly and nonlinearly coupled dispersive PDEs describing one baroclinic and two barotropic wave trains of small amplitude and large zonal wavelength in the presence of vertical and horizontal zonal shears. As in Ref. [1] nonlinear coupling occurs through baroclinic and symmetric barotropic waves and linear coupling occurs in the presence of mean shears and winds. The addition of baroclinic shears of the opposite meridional symmetry of the baroclinic waves or the addition of antisymmetric barotropic winds provides a route for energy transfer to antisymmetric barotropic waves. The small amplitude equations derived here have linear couplings, but are also strongly coupled through quadratic energy conserving nonlinearities. In fact the equations are shown to have a Hamiltonian structure and to admit analytic solitary wave solutions. Whether or not the equations admit other solitary waves solutions is an open question as is the interesting issue of their possible complete integrability.

The results of Section 5 indicate that a moderate amount of antisymmetric baroclinic mean shear serves primarily to shift the maximum of the zonal wind north of the equator. The effective energy transfer from the midlatitudes to $m = 1$ equatorial Rossby waves, which was discussed in Ref. [1] proceeds unhindered, with simply a northward shift of the centerline of the zonal mean barotropic velocity. However, a more significant antisymmetric baroclinic mean shear allows energy to be transported from symmetric barotropic waves to baroclinic waves and then to antisymmetric barotropic waves, effectively quenching the baroclinic waves. Equivalently, the centerline of the barotropic waves moves far enough north to significantly reduce the zonal barotropic wave velocity at the equator shutting down the nonlinear connection of the barotropic waves to the baroclinic waves. The effect of antisymmetric baroclinic shear on the equator to midlatitude connection is simply to shift the symmetry latitude of the resultant barotropic waves northward to coincide with that of the zonal mean velocity. Purely antisymmetric zonal shears drive largely baroclinic asymmetric waves. Given the expressions for the parameters, it is straightforward to integrate the RBSAB equations in the case of antisymmetric, $m = 2$, baroclinic waves and their resonant barotropic waves. In particular it would be interesting to compare the combined results of $m = 1, 2$ in the presence of mean shears derived from the observational record, but this task is well beyond the scope of the current work and will be reported elsewhere.

Tropical heating and midlatitude barotropic waves are important forcing mechanisms for the equatorial Rossby waves as are radiative damping and atmospheric boundary layer drag. These effects will modify the zonal mean shears over the timescales of the wave interactions and can provide a route to couple the nonresonant wave packets, a description of which would require the amplitude equations in (19) for both $m = 1, 2$ in addition to the new effects. These important additions are reported elsewhere by the authors [21].

Acknowledgments

J. A. Biello was supported by an NSF VIGRE Postdoctoral Fellowship at Rensselaer Polytechnic Institute, no. DMS-0083646. A. J. Majda is partially supported by NSF grant no. DMS-9972865, ONR grant no. N0014-96-1-0043, and an NSF-FRG grant.

Appendix A. The equivalence of Γ_A in the barotropic and baroclinic wave equations

We provide the proof that for all baroclinic shears, $\bar{U}$, Γ_A from (24) is equal to Γ_A from (27). The equivalent proofs for Γ_S and α follow the same argument and are omitted. The difference of the two coefficients is

$$\begin{aligned}
&\int_{-\infty}^{\infty} \left[-\sqrt{2} l \sin(ly)(\hat{q}+\hat{r})\bar{U} + l^2 \cos(ly)\hat{v}\bar{U} \right] dy \\
&\quad + \int_{-\infty}^{\infty} \cos(ly) \left[\left(\frac{\hat{q}+\hat{r}}{\sqrt{2}} \bar{U} \right)_y + \hat{q}\bar{Q}_y + \hat{r}\bar{R}_y \right] dy \\
&= \int_{-\infty}^{\infty} \cos(ly)[-2(\hat{u}\bar{U})_y + l^2 \hat{v}\bar{U}]\, dy \\
&\quad + \int_{-\infty}^{\infty} \cos(ly)\left[(\hat{u}\bar{U})_y + \hat{q}\bar{Q}_y + \hat{r}\bar{R}_y \right] dy \qquad \text{(A.1)}
\end{aligned}$$

where an integration by parts has been performed in the first integral and the definition $\hat{u} = \frac{\hat{q}+\hat{r}}{\sqrt{2}}$ has been used. Again using this definition and $\hat{p} = \frac{\hat{q}-\hat{r}}{\sqrt{2}}$ the quantities in braces shall be denoted I and can be simplified to

$$\begin{aligned}
I &= -2(\hat{u}\bar{U})_y + l^2\hat{v}\bar{U} + (\hat{u}\bar{U})_y + \hat{q}\bar{Q}_y + \hat{r}\bar{R}_y \\
&= l^2\hat{v}\bar{U} - (\hat{u}\bar{U})_y + \hat{u}\bar{U}_y + \hat{p}\bar{P}_y \\
&= \quad l^2\hat{v}\bar{U} - \hat{u}_y\bar{U} + \hat{p}\bar{P}_y \\
&= \quad (l^2\hat{v} - \hat{u}_y - y\hat{p})\bar{U} \qquad \text{(A.2)}
\end{aligned}$$

where the relation of geostrophic balance (17) has been used in the last line. The eigenfunctions $\hat{u}, \hat{p}$ also respect geostrophic balance and using it to eliminate the time derivatives from the linearized LWSEBB, Equation (10) with $\delta = 0$, yields

$$\hat{v}_{yy} - y^2\hat{v} + (y\hat{p} + \hat{u}_y) = 0. \tag{A.3}$$

Eliminating $\hat{u}$ and $\hat{p}$ from (A.2) we find

$$I = l^2\hat{v} + (\hat{v}_{yy} - y^2\hat{v}). \tag{A.4}$$

The right hand side of (A.4) is the defining equation for the parabolic cylinder function and because $\hat{v} \propto D_m$ and $l^2 = 2m + 1$ it is identically zero.

Appendix B. The parameters of the rescaled normal form

The canonical form in (28) is derived from BSAB in (19) through the following elementary rescalings, which follow Ref. [1]. Substituting

$$\begin{aligned} &A = A_0\hat{A}, \quad B^S = s_B B_0 \hat{B}^S, \quad B^A = s_B B_0 \hat{B}^A, \\ &x = x_0\hat{x}, \quad \text{and} \quad \tau = \tau_0\hat{\tau} \end{aligned} \tag{B.1}$$

where $s_B = \pm 1$, into (19) yields (28) with the relative dispersion given by

$$D = \frac{D_A r_B}{D_B r_A} \tag{B.2}$$

and the parameters of the barotropic wind and baroclinic shear are given by

$$\begin{aligned} \Gamma'_{A,S} &= \frac{\sqrt{r_A}}{\alpha}\Gamma_{A,S} \qquad \mu' = \frac{\sqrt{r_B}}{|\alpha|}\mu \\ \lambda' &= \frac{r_A}{|\alpha|\sqrt{r_B}}\lambda \qquad \sigma' = \frac{r_A}{|\alpha|\sqrt{r_B}}\sigma \end{aligned} \tag{B.3}$$

where the primes have been dropped in (28).

The values of the scaling parameters, A_0, B_0, s_B, x_0, and τ_0 are

$$\begin{aligned} A_0 &= \frac{1}{\sqrt{r_A}}, \qquad B_0 = \frac{1}{\sqrt{r_B}}, \\ x_0 &= \sqrt{\frac{D_B r_A}{|\alpha|\sqrt{r_B}}}, \qquad \tau_0 = \sqrt{\frac{D_B r_A^3\sqrt{r_B}}{|\alpha|^3}} \end{aligned} \tag{B.4}$$

where, to keep τ_0 positive the choice

$$s_B = \operatorname{sgn}(\alpha) \tag{B.5}$$

must be made. The explicit values of the scaling parameters are

$$(A_0, B_0, x_0, \tau_0, s_B) = \begin{cases} (0.61, 0.43, 0.60, 1.97, 1) & \text{for } m = 1 \\ (0.58, 0.38, 0.55, 4.22, -1) & \text{for } m = 2. \end{cases} \tag{B.6}$$

References

1. A. Majda and J. A. Biello, The nonlinear interaction of barotropic and equatorial baroclinic rossby waves, *J. Atmos. Sci* 60:1809–1821 (2003).
2. P. J. Webster, Response of the tropical atmosphere to local steady forcing, *Mon. Weather Rev.* 100:518–541 (1972).
3. P. J. Webster, Mechanisms determining the atmosphere response to sea surface temperature anomalies, *J. Atmos. Sci*. 38:554–571 (1981).
4. P. J. Webster, Seasonality in the local and remote atmospheric response to sea surface temperature anomalies, *J. Atmos. Sci.* 39:41–52 (1982).
5. A. Kasahara and P. L. Silva Dias, Response of planetary waves to stationary tropical heating in a global atmosphere with meridional and vertical shear, *J. Atmos. Sci.*, 43:1893–1911 (1986).
6. B. J. Hoskins and F.-F. Jin, The initial value problem for tropical perturbations to a baroclinic atmosphere, *Quart J. Roy. Meteor. Soc.* 117:299–317 (1991).
7. B. Wang and X. Xie, Low frequency equatorial waves in vertically sheared zonal flow: 1. Stable Waves, *J. Atmos. Sci.* 53:449–467 (1996).
8. H. Lim and C. P. Chang, A theory for midlatitude forcing of tropical motions during winter monsoons, *J. Atmos. Sci.* 38:2377–2392 (1981).
9. H. Lim and C. P. Chang, Generation of internal mode and external mode motions from internal heating: Effects of vertical shear and damping, *J. Atmos. Sci.* 43:948–957 (1986).
10. B. J. Hoskins and G.-Y. Yang, The equatorial response to higher latitude forcing, *J. Atmos. Sci.* 57:1197–1213 (2000).
11. J. W.-B. Lin, J. D. Neelin and N. Zeng, Maintenance of tropical intraseasonal variability: Impact of evaporation-wind feedback and midlatitude storms, *J. Atmos Sci.* 57:2793–2823 (2000).
12. H. Mitsudera, Eady solitary waves: A theory of type B cyclogenesis, *J. Atmos. Sci.* 51:3137–3153 (1994).
13. G. Gottwald and R. Grimshaw, The formation of coherent structures in the context of blocking, *J. Atmos. Sci.* 56:3640–3662 (1999).
14. J. D. Neelin and N. Zeng, A quasi-equilibrium tropical circulation model - Formulation, *J. Atmos. Sci.* 57:1741–1766 (2000).
15. A. Majda and M. Shefter, Models for stratiform instability and convectively coupled waves, *J. Atmos. Sci.* 58:1567–1584 (2001).
16. W. A. Heckley and A. E. Gill, Some simple analytical solutions to the problem of forced equatorial long waves, *Q. J. R. Meteor. Soc.* 110:203–217 (1984).
17. A. Majda, *Introduction to PDE's and Waves for the Atmosphere and Ocean*, p. 234, American Mathematical Society, RI, 2003.
18. J. P. Boyd, Equatorial solitary waves. Part I: Rossby solitons, *J. Phys. Oceanogr.* 10:1699–1717 (1980).

19. A. Patoine and T. Warn, The interaction of long quasi-stationary waves with topography, *J. Atmos. Sci.* 39:1018–1025 (1981).

20. A. Majda and R. Klein, Systematic multiscale models for the tropics, *J. Atmos. Sci.* 60:393–408 (2003).

21. J. A. Biello and A. Majda, 2003: The effect of boundary layer dissipation and radiative damping on equatorial baroclinic and barotropic Rossby waves, *Geophys Astrophys Fluid Dyn.*, in press.

Courant Institute of Mathematical Sciences

(Received July 16, 2003)